

No. 71 August 2024

# STEEL CONSTRUCTION

TODAY & TOMORROW

<https://www.jisf.or.jp/en/activity/sctt/index.html>

*Feature Article*

## Technologies to Reinforce and Make Resilient Foundation Structures

- 1 Development of Method to Reinforce Gravity-type Breakwaters Employing Steel Piles
- 5 Secondary Design Method for Building Foundations Capitalizing on the Deformation Capacity of Steel Pipe Piles
- 7 New Development in Construction Management in the Hammer Driving of Steel Pipe Piles
- 9 Research on Additional Piling Method for Pile Foundations of Road Bridges
- 11 Model Experiments on Piping Failure of River Levees
- 13 Low-carbon Measures in the Life Cycle of Concrete Structures
- 19 JISF Operations  
AJSI Webinar 2024  
Japan-Thailand Steel Cooperation Program

*Published Jointly by*



The Japan Iron and Steel Federation



Japanese Society of Steel Construction

# Development of Method to Reinforce Gravity-type Breakwaters Employing Steel Piles

**Yoshiaki Kikuchi**  
Coastal Development Institute of Technology

## Need for Highly Resilient Breakwaters

The coastal area of the Tohoku district has been frequently attacked by tsunamis for a long time. Consequently, as a tsunami countermeasure in the district, tsunami breakwaters have been constructed at the mouth of bays where ports are located.

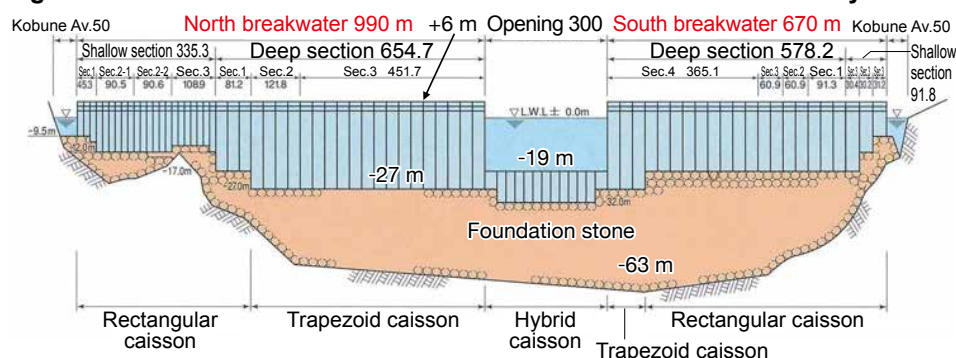
As a typical example of tsunami breakwaters, a breakwater constructed in the Kamaishi Bay is introduced. As shown in Fig. 1, as much as 95% of the bay mouth was shut with mounds and caissons of the breakwater so as to suppress the intrusion of seawater into the bay. Further, the dimensions of stone materials and the caisson used there were designed with reference to the maximum-scale tsunamis that have landed in the past. Notwithstanding, the tsunamis that landed in March 2011 surpassed those in the past in terms of scale, and as a result more than 80% of this breakwater suffered damage from these tsunamis (Fig. 2).

In a gravity-type breakwater in which large caissons are mounted on the mound, the caisson is structured in ways that secure its stability to the wave force-induced horizontal forces with the friction resistance demonstrated in the lower surface of the caisson (see Fig. 3). As can be understood from this, because it is required for the caisson to be designed usually to satisfy the balance of horizontal forces, if a horizontal force surpassing that as-



**Dr. Yoshiaki Kikuchi:** After graduating from the Graduate School of the University of Tokyo, he entered the Ministry of Transport and was assigned to Port and Harbour Research Institute in 1983. Then he moved to Tokyo University of Science as a professor in 2012. He assumed his current position as councilor of Coastal Development Institute of Technology in 2024.

**Fig. 1 Sectional Profile of the Breakwater at the Mouth of Kamaishi Bay**



Source of data: Kamaishi Port Office, Tohoku Regional Development Bureau, Ministry of Land, Infrastructure, Transport and Tourism

sumed in the design stage works on the caisson, its stability cannot be ensured.

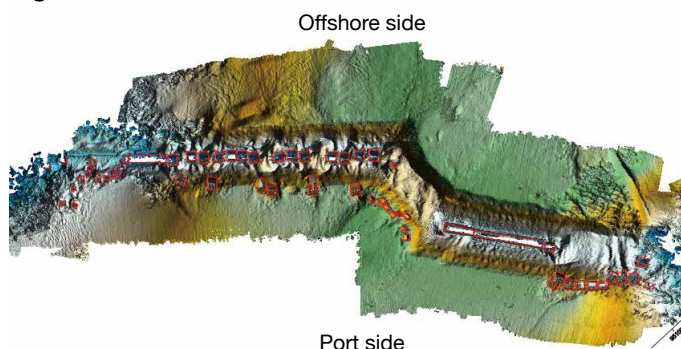
As can be seen from the tsunami disaster in March 2011, a structure that is damaged at once when an external force surpassing assumed levels works is insufficient as a countermeasure against natural disasters. In light of this situation, it was proposed to construct a breakwater that is resilient or that will not easily suffer damage, even when an external force surpassing assumed levels strikes.

## Tsunami-induced Suffering Mechanism and Countermeasures

Another reason attributable to the suffer-

ing of damage at bay mouth breakwaters is that tsunamis overflowed the caisson to cause scouring of the mound behind the caisson. It was shown in a hydraulic experiment conducted by the Port and Airport Research Institute (PARI)<sup>1)</sup> that, when the mound was scoured due to overflowing, the caisson became unstable at once in a certain timing, thereby leading to collapse. It was desired from this experiment that, in order to improve tsunami resistance, not only should horizontal resistance be enhanced but scouring of the mound behind the caisson should also be prevented from occurring.

**Fig. 2 Movement of Caissons and Deformation of Mounds**



Source of data: Ministry of Land, Infrastructure, Transport and Tourism

**Fig. 3 Stability of Caissons Applied for Breakwaters Is Determined by Sliding Resistance**

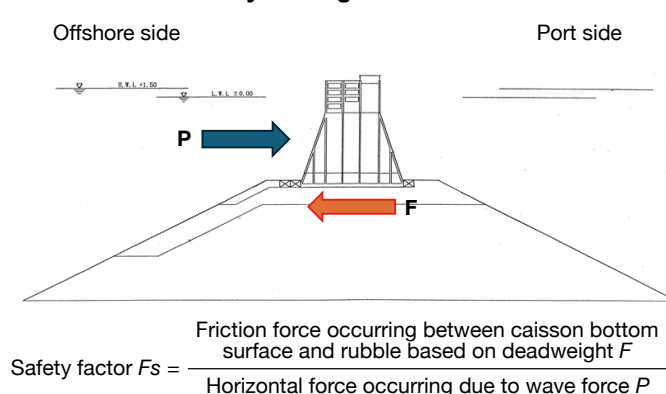
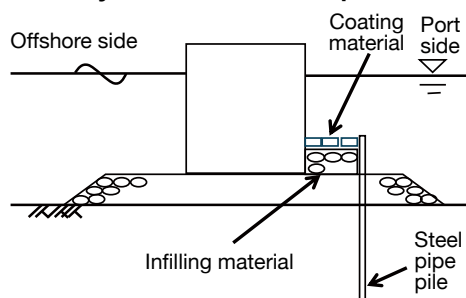




Fig. 4 shows an image of a breakwater reinforced by the use of steel pipe piles, which was proposed to meet the above-mentioned need. The premise of this proposal was that a certain level of horizontal movements should be allowed for the caisson. When a horizontal force works on the breakwater and the mound behind the caisson is scoured, it is forecast that the entire tsunami breakwater structure will show the displacement behavior shown in Fig. 5. But, as can be understood from the figure, the passive resistance of the ground behind the pile can be expected due to the deflection of the pile, and the increment of the horizontal force from the use of the pile cannot be expected when the pile is not deflected.

In other words, this reinforcing method can be applied only to structures having large allowable displacement, such as a breakwater. Further, in this reinforced

**Fig. 4 Image of Breakwater Reinforced by the Use of Steel Pipe Pile**



**Fig. 5 Behavior of Entire Breakwater System in the Event of Tsunami Attack**

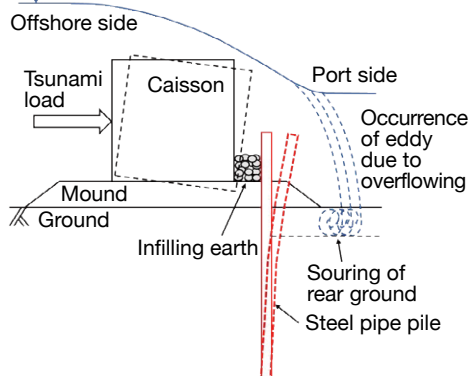
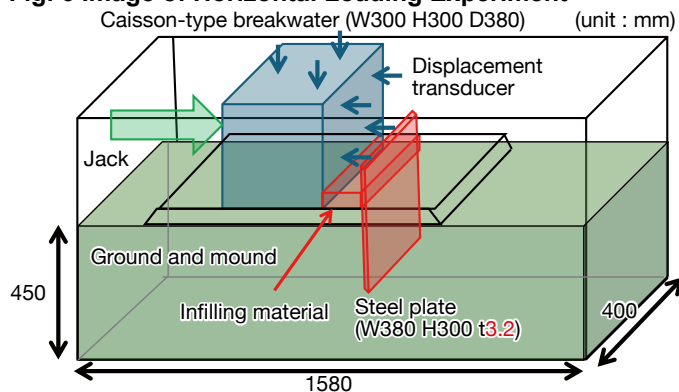


**Fig. 6 Image of Horizontal Loading Experiment**



structure, the pipe pile is not driven just behind the caisson but driven with a certain separation to provide infilling between the caisson and the pile. The aim of this pile driving system is to reduce the maximum bending moment working on the pile by dispersing the load working on the pile.

Incidentally, regarding the scouring of the rear ground, while the ground further behind the pile is scoured as seen in Fig. 5, it is expected that scouring is less likely to occur between the pile and the caisson. Photo 1 shows scouring of the rear ground in the hydraulic experiment conducted at PARI, from which it is understood that scouring did not occur at the range sandwiched between the pile and the caisson.

### Effects of New Reinforcing Method

In order to examine the effect and impact when the caisson is reinforced with piles, at first it is necessary to confirm the following seven factors<sup>2) 3)</sup>: effect of pile application, separation between pile and caisson, height of infilling, rigidity of piles, embedding length of piles, interval between piles, and scouring behind the piles.

A horizontal loading experiment was conducted on two of the above-mentioned seven factors: the effect of pile application and the rigidity of pile, the results of which are reported below.

Fig. 6 shows an image of the loading experiment that was conducted. The sand box used in the experiment measured 40 cm in width and 158 cm in length, and a steel box, mass of which was adjusted to 70 kg by sand, was adopted as the caisson. The length of the caisson (width direction of the earth tank) was set at 38 cm. The width of the caisson (length direction of the earth tank) was set at 30 cm with an

image prepared at a scale of 1/60 of the practical structure. Dry silica sand No. 5 was used for the model ground, and the relative density of the ground was set at 80%. Gravel was used as the infilling material. In the experiment, two steel plates 3.2 and 1.2 mm in thickness (embedded length: 28 cm) were used in place of a steel pile.

Fig. 7 shows the experimental results. In the case of reinforcement by means of backfilling, backfilling was provided with a crest width of 3 cm behind the caisson, a height of 15 cm and a slope of 1:1.5 and by the use of gravels. In the case of reinforcement by steel plate, the separation from the caisson at the stage of reinforcement with steel piles was set at 5 cm. As can be understood from the figure, the horizontal resistance in the backfilling reinforcement method became slightly larger than that in the non-reinforced method, but its effect was limited.

On the other hand, in the case of reinforcement by the use of steel piles, it is forecast that the horizontal resistance far larger than that in the backfilling reinforcement method can be obtained, and further the effect in which the resistance increases along with the displacement of the caisson is significant. Photo 2 shows the deformation of the caisson within the ground in the case of reinforcement with the steel piles. In the case of non-reinforcement or reinforcement by means of backfilling, while the caisson showed displacement only in the form of sliding on the ground under the current loading experimental conditions, the caisson also showed the behavior of sinking into the ground due to reinforcement with steel piles, and thus it was understood that the collapse mode of the caisson also changed.

By the way, the lifeline in the case of

Photo: Port and Airport Research Institute



Photo1 Scouring of the ground behind the breakwater reinforced by the use of steel pile

reinforcing a structure is whether or not the reinforcing member collapses, and thus in the case of reinforcement with steel piles, it is important for the pile to cause no buckling or falling down. That is, it is important how the embedding length and the cross section of the pile are designed.

Specifically, while the weight and dimension of the caisson are decided by the wave force and other conditions, it is necessary to change the cross section of the pile according to the ground condition in addition to the wave force. In order to simplify the experimental conditions, because of the simplicity of the experiment conducted on sandy ground,

it was decided to also conduct the experiment on sandy ground, but in order to work out the condition in which the ground is relatively weak, it was decided to work out the effect of the weak ground by changing the weight of the caisson.

In other words, the experiment was conducted with the collapse pattern of the caisson changed to several patterns by changing not only the ground density but also the caisson weight, and examinations were made of how the distribution of the load working on the pile changed depending on the fracture mode of the caisson<sup>4)</sup>.

Fig. 8 shows an image of the experiment used for the design of the pile cross

section. The earth tank applied was the same as that in Fig. 6, and the ground material applied was the same as that in Fig. 6 (silica sand No. 5, gravel). The relative density of the ground (layer thickness: 55 cm) applied was 10% and 80%. The steel box applied as the caisson was the same, but its weight was adjusted to 115 kg and 24 kg. The separation between the pile and the caisson was 5 cm. For this experiment, a total of 12 rectangular piles (steel, 3 cm in width, 2.3 mm in thickness) were applied, and the embedding length was set at 55 cm. The reason why the embedding length was increased in this experiment was to reproduce conditions in which the embedding length is long so that the experimental results could easily be assessed.

In the examination of experimental results, the bending moment distribution observed in steel piles was first obtained. Based on this, the deflection distribution was found by means of calculation via second integration and division by flexural rigidity, while the ground reaction force distribution was found by a second derivative. The ground reaction force distribution that was found in this analysis referred to the differences in loads working on both sides of the piles. Actually, however, the aim of this examination was to learn how much load was working on the piles from the caisson. Therefore, the degree of external force working from the caisson was estimated by subtracting the ground reaction force from the load distribution found by the derivative, as imaged in Fig. 9.

This external force distribution took complex forms depending on the conditions. This examination focused on the case of the shape approximating a trian-

**Fig. 7 Effect of Reinforcement by the Use of Steel Plate**

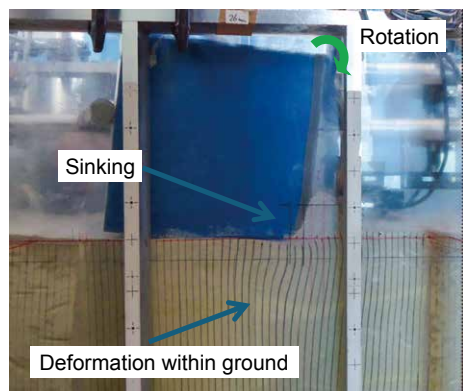
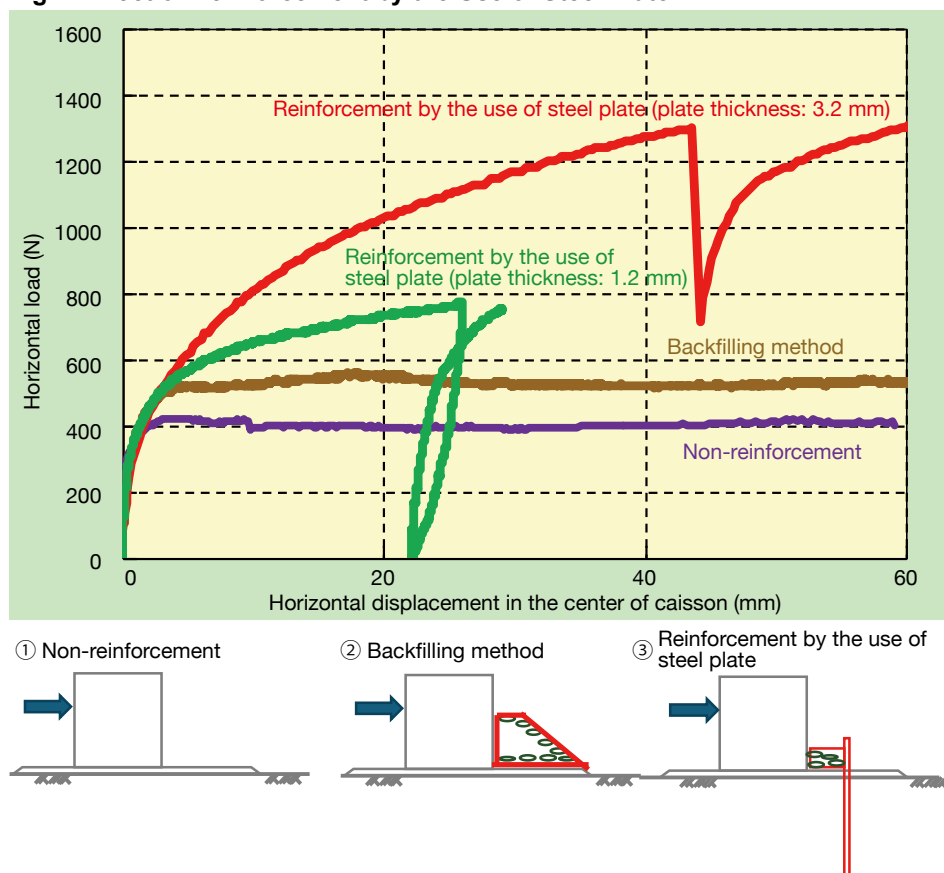
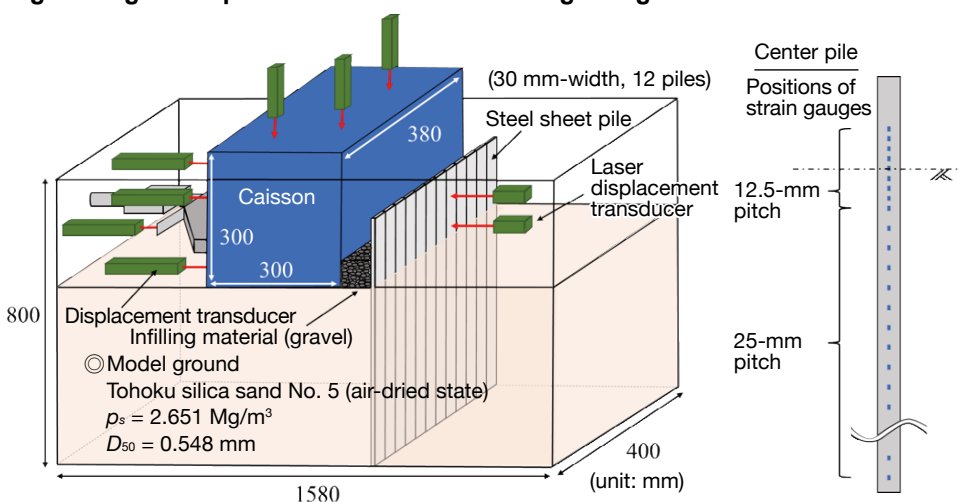


**Photo 2 Behaviors of the caisson and the ground in the case of reinforcement by the use of steel plate**

**Fig. 8 Image of Experiment Used for Examining Design of Pile Cross Section**



gle; how this would affect the bending moment distribution and the deflection distribution as obtained by calculation. The result of this comparison is as shown in Fig. 10. The conditions applied in this loading experiment were: a caisson mass of 115 kg; the ground relative density of 80%; and the horizontal loads used to work on the caisson being 600N, 800N and 1,000N, respectively.

In order to approximate the shape of the external force distribution to a triangle, a decision was made to adopt the top position of infilling soil as the upper end of a triangle and the first 0 point depth of pile deflection as the lower end of a triangle, where the area of the triangle coincided with the load applied to work on the caisson. As is clear from Fig. 10, it was revealed that the experimental results were also largely reproducible through approximating the shape to a triangle.

## Tasks in Application

Several tasks involved in applying the newly-developed breakwater reinforcing method with steel piles are cited below.

Because this breakwater reinforcement method involves the horizontal resistance of the ground being expected to work, if a certain level of horizontal force cannot be expected for the ground, it is difficult for the method to demonstrate its effect. In light of this, it is considered that this reinforcement method is rather unsuitable for clayey ground. In addition, when this method is applied to a newly constructed breakwater, care needs to be given to bending of the pile under construction. Further, in the case of applying to an existing breakwater, it is required to drive the pile into the mound.

As to the task of whether the pile can be driven into rubble ground like a mound, this possibility has definitely been examined, and it has been confirmed that the pile can be driven into the rubble ground by using a special pile driving method<sup>5)</sup>.

## References

- 1) Taro Arikawa, Masaharu Sato, Kenichiro Shimosako, Takashi Tomita, Gyeong-Seon Yeom, Tatsuya Niwa: Failure Mechanism and Resiliency of Breakwaters under Tsunami, Technical Note of The Port and Airport Research Institute No.1269, 37p., 2013.
- 2) Motohiro Suguro, Yoshiaki Kikuchi, Taichi Hyodo, Masatsugu Kiko, Soichiro Nagasawa, Shunsuke Moriyasu, Shin Oikawa: Horizontal Loading Experiment on Breakwater Reinforced by Steel Pipe Piles, Journal of Japan Society of Civil Engineers, Ser. B3 (Ocean Engineering), Vol. 71 Issue 2, pp. I\_617-I\_622, 2015. DOI [https://doi.org/10.2208/jscejoe.71.I\\_617](https://doi.org/10.2208/jscejoe.71.I_617)
- 3) Motohiro Suguro, Yoshiaki Kikuchi, Taichi Hyodo, Yutaro Yamazaki, Sayako Tamaki, Shunsuke Moriyasu, Shin Oikawa: Effect of Flexural Rigidity of Piles on Horizontal Resistance of Reinforced Gravity Type Breakwater with Steel Pipe Piles, Journal of Japan Society of Civil Engineers, Ser. B3 (Ocean Engineering), Vol. 72 Issue 2, pp. I\_241-I\_246, 2016. DOI [https://doi.org/10.2208/jscejoe.72.I\\_241](https://doi.org/10.2208/jscejoe.72.I_241)
- 4) Kentaro Ichinose, Yoshiaki Kikuchi, Yusuke Mochida, Shin Oikawa: Distribution of External Forces Acting on the Piles of a Gravity Type Breakwater Reinforced with Steel Pipe Piles, Japanese Journal of JSCE, Vol. 79 Issue 18, Article ID: 23-18142, 2023. DOI <https://doi.org/10.2208/jscejj.23-18142>
- 5) Shunsuke Moriyasu, Ryuta Tanaka, Shin Oikawa, Masato Tsujii, Shinji Taenaka, Kazuo Kubota, Noriyoshi, Harata: Development of New Type of Breakwater Reinforced with Steel Piles against a Huge Tsunami, Nippon Steel and Sumitomo Metal Technical Report, No.403, pp.63-69, 2015.

**Fig. 9 Concept of External Force Working on Pile from Offshore Side**

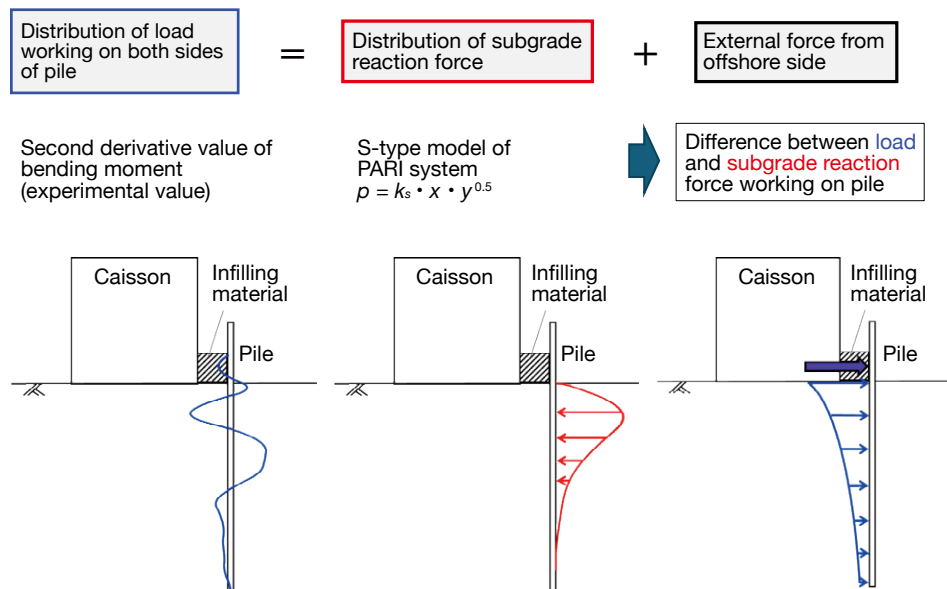
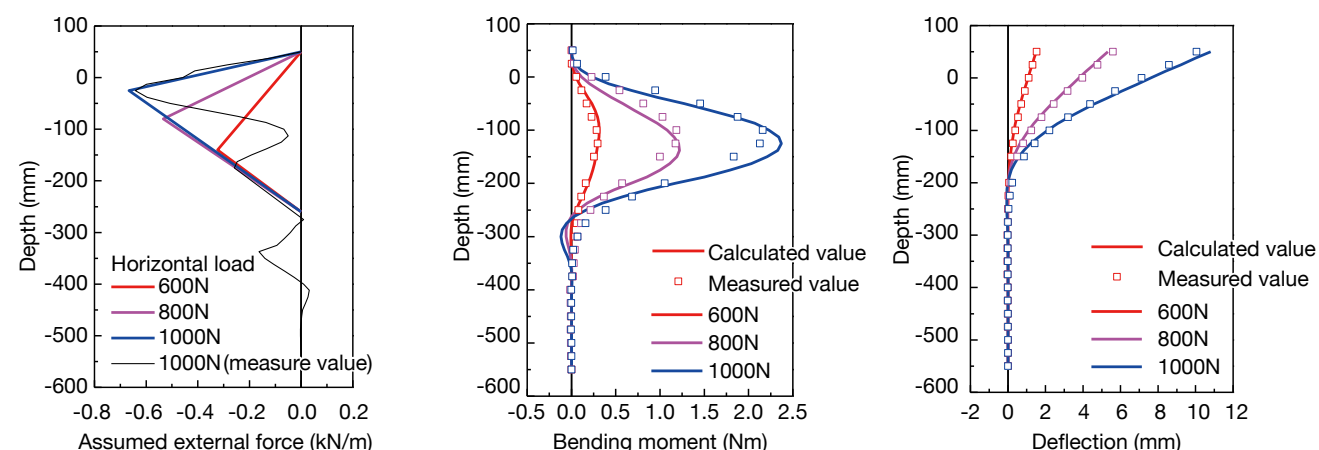


**Fig. 10 Confirmation of Validity of Approximated External Force Distribution**





# Secondary Design Method for Building Foundations Capitalizing on the Deformation Capacity of Steel Pipe Piles

**Katsuichiro Hijikata**

Former Professor, Shibaura Institute of Technology



**Katsuichiro Hijikata:** After finishing the School of Engineering, The University of Tokyo, he entered Tokyo Electric Power Co., Inc. in 1981. He obtained a doctor's degree in engineering from The University of Tokyo in 1991. Then he became professor at the Shibaura Institute of Technology in 2013. He is currently part-time instructor of the Shibaura Institute of Technology.

## Need for Examination of Secondary Design

In the Building Standard Law of Japan, while the secondary design of building foundations structures is not prescribed, a trend towards the adoption of secondary design is growing in both public and private sectors from the perspectives of business continuity plans and asset protection. In the *Recommendations for Design of Building Foundations* of the Architectural Institute of Japan (*AIJ Recommendations*) revised in 2019, the secondary design method for building foundations was shown.

Given this situation, a research project commissioned by the Japan Iron and Steel Federation was started at the Japanese Society of Steel Construction (JSSC). Specifically, the Research Group on Structuring Secondary Design Methods for Steel Pipe Piles for Building Foundations was established within JSSC, which promoted the examination of secondary design methods employing steel pipe piles and concrete-filled steel tube (CFT) piles in the two years from 2019.

## Course of Examinations

The Research Group directed its research

efforts towards establishing a secondary design method that capitalizes on the characteristic property of steel pipe piles and CFT piles of being high in toughness, and promoted examinations in accordance with the following course:

- For level 2 seismic loads, it was confirmed how much the strength of foundations is improved in the case of setting limit values for steel pipe piles and CFT piles as “limit deformation” compared to the case of setting limit values for steel pipe piles and CFT piles as “limit strength.” Fig. 1 shows the definition of limit strength and limit deformation of steel pipe piles and CFT piles. In this examination, “limit strength” was defined as a state in which one of group piles reaches the limit strength, and “limit deformation” was defined as a state in which one of group piles reaches the limit deformation (limit curvature) or two-point hinges occurred in one pile.
- For the relationship between the moment and the curvature of steel pipe piles ( $M-\phi$  relationship) used in this examination, the assessment formulae shown in the *AIJ Recommendations* was adopted. For the relationship between the moment and the

curvature of CFT piles ( $M-\phi$  relationship), an assessment formulae was adopted that was revised by the JSSC's Research Group based on the *Recommendations for Design and Construction of Concrete Filled Steel Tube Structures* of AIJ.

- In the calculation of the stress occurring in the pile, the “Group Pile Frame Model” shown in the *AIJ Recommendations* was applied. In this calculation method, one row of group piles and foundation beams was modeled, on which the building inertia force and the ground displacement are simultaneously worked (refer to Fig. 2), and it is

**Fig. 2 Outline of Group Pile Frame**

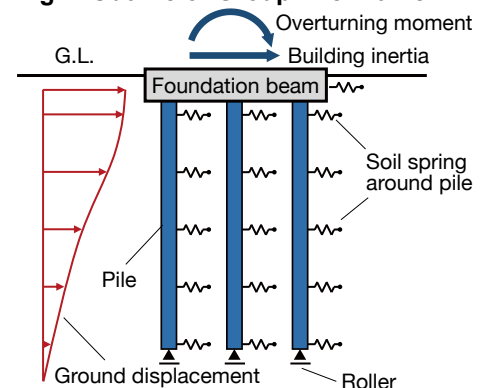
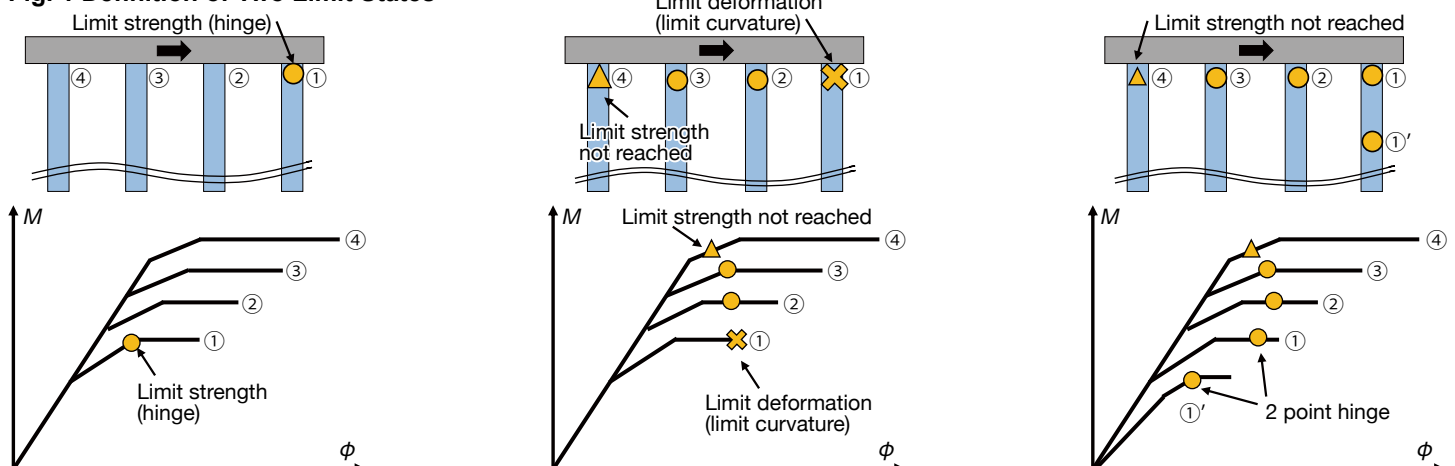


**Fig. 1 Definition of Two Limit States**



- possible to take into account the nonlinearity of the pile structure and the ground.
- The target subjected to examination was a steel-structure hospital building with 5 floors and a total floor area of about 5,000 m<sup>2</sup>. Fig. 3 shows the soil condition, and Fig. 4 the pile placement. The ground was assumed to be located in the coastal area of Japan. The pile length was 21 m, and the upper part was structured with CFT piles, and the lower part with steel pipe piles. The cross section of piles was set based on an appropriate level 2 seismic load and in conformity with currently prevailing practice. The diameter of the piles ranged from 900 mm to 1,200 mm.
  - Analysis was made in ways that proportionally increase the building's inertia force and the ground displacement and work them on the group pile frame model to find the load at which the pile reaches the limit strength and limit deformation.

### Examination Results

Fig. 5 shows the relationship between the horizontal load working on the group pile frame model  $Q$  (building's inertia force) pertaining to the group pile in row X2 as shown in Fig. 4 and the displacement  $\delta$ . The horizontal load at which the pile reaches the state of limit deformation showed an increase of 1.69 times the horizontal load at which the pile reaches the state of limit strength (1.77/1.05), where the figure shown in parenthesis is the ratio to the level 2 seismic load.

Fig. 6 shows the formation of hinges at each pile. It was confirmed that, at first the hinge occurred in the head of the Y1 pile, where its limit value reached the limit strength, then the hinge occurred in each pile head one after another, and finally the hinge occurred in the underground section of the Y3 pile, where its limit value reached the limit deformation.

### Useful Results

In the above examination, it was confirmed that the horizontal load borne by the group pile frame sharply increased by setting the criteria on the "limit deformation," compared to the case of setting the criteria on the "limit strength." This is a useful knowledge that will lead

to the rational design of steel pipe piles and CFT piles.

A full version of the examination results was published in the "Technical Explanations pertaining to Secondary Design Methods for Steel Pipe Piles for Building Foundations" in *JSSC Technical Report* (No. 127, August 2022).

**Fig. 3 Soil Condition (N-Value)**

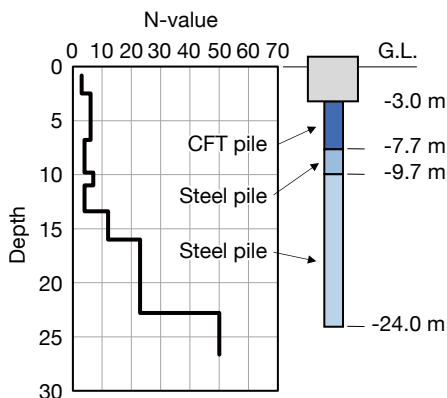


**Fig. 4 Pile Placement**

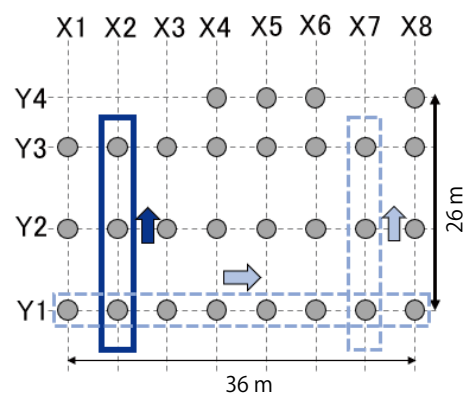


**Fig. 5 Q- $\delta$  Relationship of Group Pile Frame**

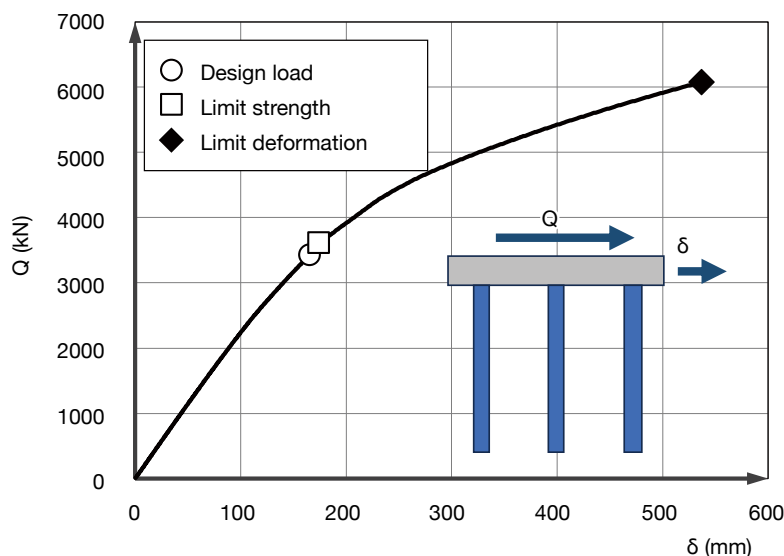
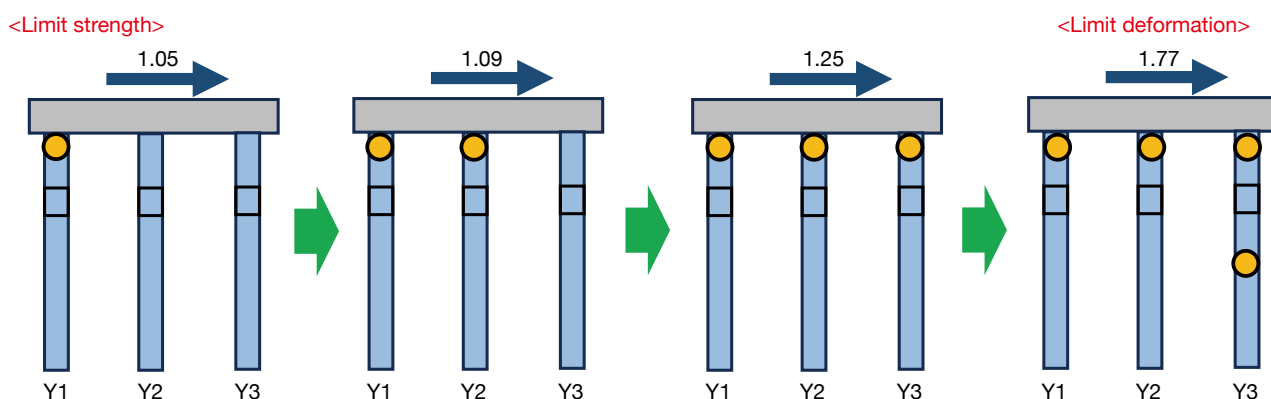


**Fig. 6 Hinge Formation Process**



# New Development in Construction Management in the Hammer Driving of Steel Pipe Piles

**Takaaki Mizutani**  
Port and Airport Research Institute

**Takaaki Mizutani:** He obtained a doctor's degree in engineering from The University of Tokyo in 2000. Then he has worked at the Port and Airport Research Institute. He currently serves as researcher of the Institute's Geotechnical Engineering Department. (In 2006-2007, he worked at Kansai International Airport Co., Ltd.)

## Need for Automated Measurement and Streamlined Construction Management

In the construction of port and harbor facilities in Japan, long, large-diameter steel pipe piles have been used extensively. High marine construction efficiency and high bearing capacity can be obtained from the use of steel pipe piles, and thus these piles are commonly driven by the use of hydraulic hammers. Execution control in pile driving is undertaken based on the  $R_d$  obtained from the following formulae that has been simplified from Hiley's Formula.

$$R_d = \frac{0.5F}{S + \frac{K}{2}}$$

where

$F$ : Blow energy

$S$ : Amount of penetration per blow

$K$ : Amount of rebound per blow

$S$  and  $K$  are measured by operating the hydraulic hammer under conditions where paper is pasted on the pile and the worker fixes by pencil (Photo 1).

However, this measurement method offers some problems: dangerous work in which the worker enters under the hammer, and the risk that the recording paper may be stained or lost. Further, the reading of recorded data and the input of this data into computers take a lot of time. In light of this, there is a strong call to further promote not only automated

measurement but streamlined construction management method.

## Two Main Purposes in Piling Construction Management

Two main purposes are cited for construction management in steel pipe pile driving.

One is to confirm that the pile tip has reached the bearing stratum. For that purpose, it is necessary to select a value corresponding to the change in the soil layer (for example, the change in the SPT-N value) as the value to be used for construction control and then to obtain these values continuously in the depth direction.

Another is to detect the defective piles. When multiple steel pipe piles are driven at an identical construction site, the bearing capacity of the respective piles will show variation due to the depth of the bearing layers and local changes in soil properties, and thus there may arise cases in which a defective pile occurs. In order to securely detect the defective pile, it is important that the variation in the values for construction control itself is low.

As a mechanism to obtain a construction control value that appropriately satisfies the two purposes mentioned above, it has been examined to use an insertion pipe with sensors to measure the amount of blow energy and penetration between the pile and the hammer (Fig. 1). This method is expected to

help automate the measurement and streamline construction management.

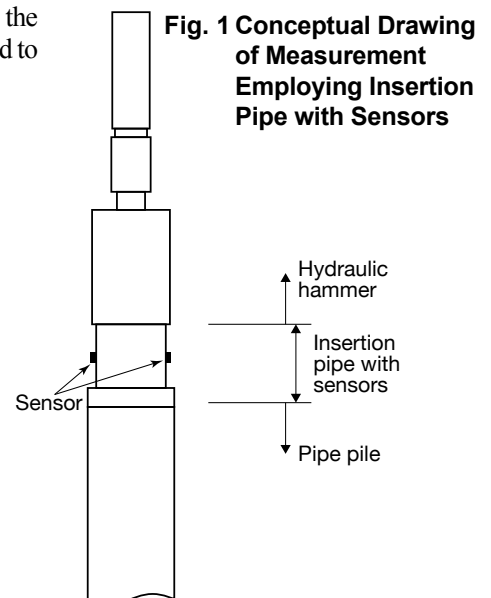
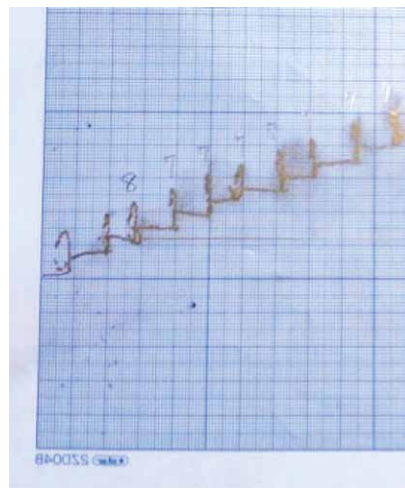
## Unification of Pile Driving Procedure

In order to perform highly reliable construction control, it is also important that the method and procedure applied for pile driving be unified. Even when the piling sites and soil properties are identical and piles with identical dimensions are applied, if a unified driving procedure is not adopted, the relative comparison of construction control values becomes difficult, which thus makes it difficult to detect the occurrence of defective piles. In particular, it is empirically known that the effect of blow energy on execution control is large. Given this, during pier-supporting pile driving at Nagoya Port, hammering was performed by controlling the blow energy of hydraulic hammer.

The horizontal axis in Fig. 2 shows the pile number, and the vertical axis the blow energy. In the figure, the data are divided into four depth sections just before 1 meter from the pile embedded depth, and the average blow energy in each section is shown. It can be confirmed from this figure that all piles within an identical depth section could be driven with an identical



Photo 1 Measurement of penetration and rebound





blow energy, excluding partial piles.  
Fig. 3 shows the penetration condition of each pile, where the horizontal ax-

is shows the pile number, and the vertical axis the penetration per blow. As with Fig. 2, the data are divided into four depth sec-

tions just before 1 meter from the pile embedded depth, and the average penetration per blow in each section is shown. A clear tendency can be seen from the figure that the penetration per blow of each pile decreases from the left side toward the right side in the figure, even though the piles are driven with an identical blow energy.

Regarding the composition of the soil layers in this area, while there is a slight difference in the surface layer between the right and left sides of the figure, the bearing layer is composed of an identical soil layer (Fig. 4). It is supposed that the pile penetration resistance near the pile embedded depth may have changed due to a gradual change of the soil properties of the bearing layer itself from the left side toward the right side in the figure.

When looking again at Fig. 3, there are piles, such as pile No. 39 in the B2 site, that has a penetration amount larger than that of its neighboring piles. In performing appropriate construction control for pile driving, it is considered necessary to pay attention to such piles. It should be noted that at this site, all piles were confirmed to have sufficient bearing capacity through pile loading tests and other means.

## Toward a New Pile Driving Method

We have a plan to perform on-site tests for the measurement of blow energy and the amount of penetration employing an insertion pipe with sensors. At the same time, we will continue to promote discussions on the unification of pile driving procedures and further examine whether certain standards for construction management in steel pipe pile driving can be established.

**Fig. 2 Results of Measurement of Blow Energy**

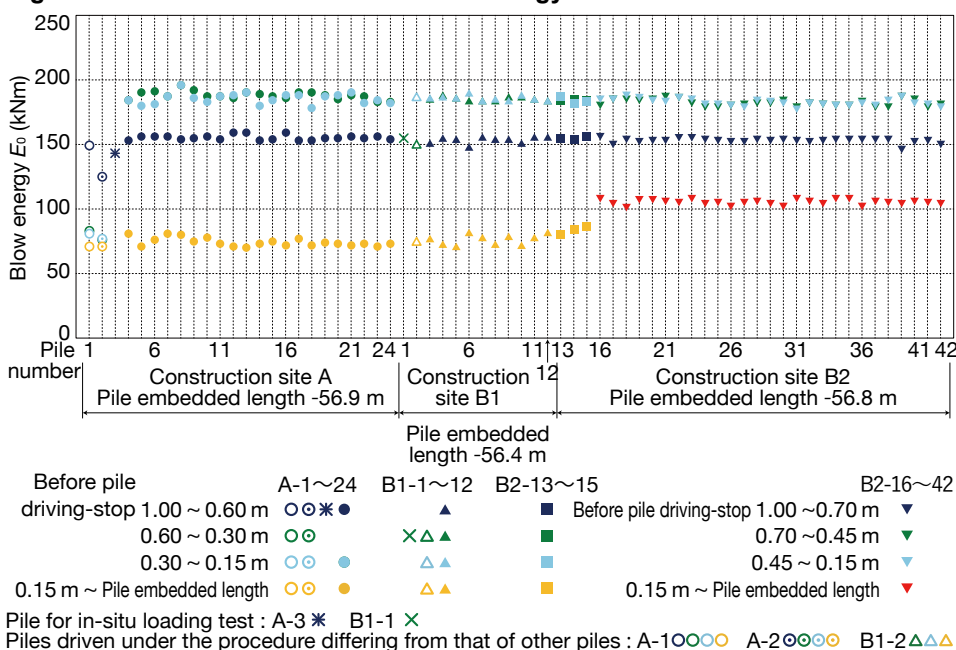


**Fig. 3 Results of Measurement of Amount of Penetration per Blow**

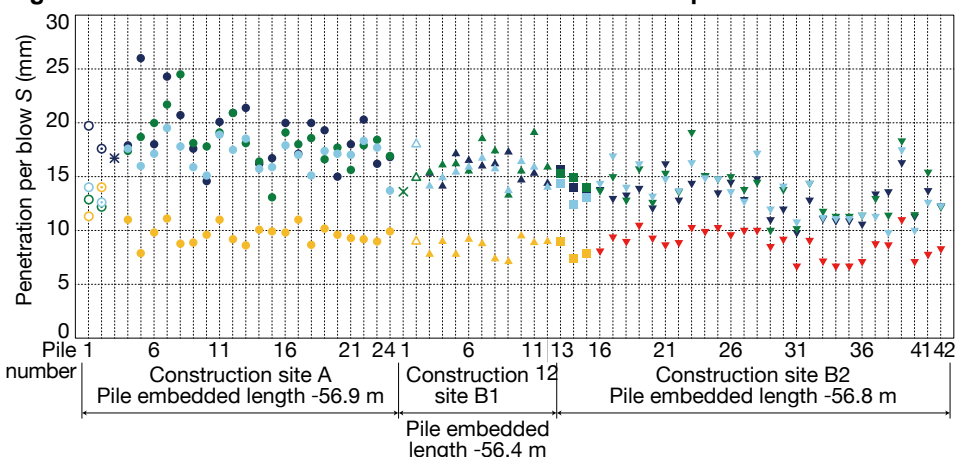
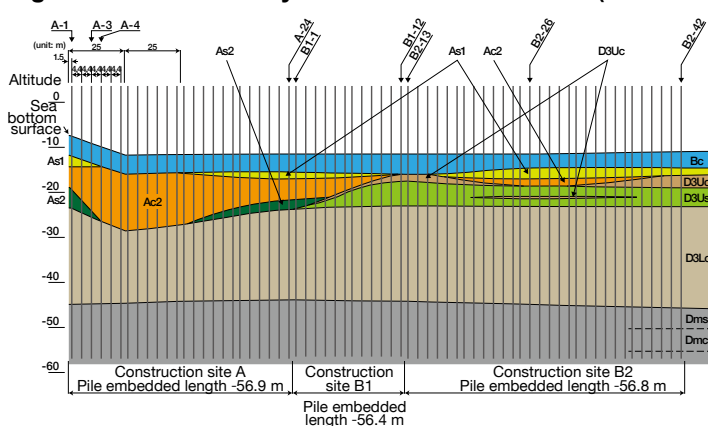


**Fig. 4 Profile of Soil Layers on Construction Site (Pile Bearing Layer: Dms Layer)**



Name of soil layer	Type of soil	STP-N value (average)	Description
As1	Medium soil Silt-mixed fine sand Silty fine sand	1-22 (8)	Sand containing fine grain, mixed sandy soil containing nearly no fine grain Silt thin layer, mixing of shell piece
Ac2	Sandy silt Silty clay	1-4 (2)	Mostly homogenous clayey soil Shell piece, thin fine-sand layer, containing plant piece
As2	Silty sand Clayey sand Sand	4-25 (11)	Mainly sand containing a slightly higher amount of fine grain Rarely thin sandy silt layer, containing sub-pebble gravel with grain diameter of 7 mm or less Partial mixing of shell piece
D3Uc	Silt Tuffaceous silt	6-19 (11)	Mainly tuffaceous clay soil Partially consolidated into gravel state Mostly uniform but partially sandwiching gravel and thin sandy layer with thickness of about 1 cm
D3Us	Silty fine sand Silt-mixed fine sand Fine sand	19-50 (41)	Composed of sand containing a slightly higher amount of fine grain and sand containing no fine grain Partially containing gravel with grain diameter of 7 mm or less
D3Lc	Silt Clay Silty clay	4-20 (10)	Homogeneous clayey soil, containing a slightly higher amount of sand and sandy silty state in upper layer Entirely shell piece, containing organic substance Slightly containing sand in block state
Dms	Silt-mixed sand Silty sand Fine sand and medium sand	11-50 (38)	Sand containing a slightly higher amount of fine grain in upper layer and sandwiching thin silty layer Sand containing a slightly higher amount of fine grain in lower layer and mostly homogenous Gravel in part of lower layer, sandwiching thin silty layer
Dmc	Sandy silt	13-22 (16)	Soil layer confirmed at partial survey sites Mostly homogenous sandy silt and increasing fine grain downward Partially sandwiching volcanic ash layer

# Research on Additional Piling Method for Pile Foundations of Road Bridges

**Kodai Takimoto**  
Public Works Research Institute



**Kodai Takimoto:** After finishing the master's course at the Graduate School of Engineering, Tohoku University, he entered the Ministry of Land, Infrastructure, Transport and Tourism (MLIT) in 2016. He worked at the Kumamoto Earthquake Recovery Div. of National Institute for Land and Infrastructure Management, MLIT in 2018 and he assumed his current position as senior researcher, Center for Advanced Engineering Structural Assessment and Research, Public Works Research Institute. His specialized field is structural engineering.

It is required for highway administrators to examine the need or no need for reinforcing highway bridge foundations taking into account the structural safety demonstrated by the existing highway bridges and the traffic function required for the road in the event of an earthquake and other disasters.

In light of this, the following article introduces the tasks in the case of applying additional piling methods used to reinforce the pile foundations of existing highway bridges and examples of related research promoted at the Public Works Research Institute.

## Widening of Footings

In most cases of the applying additional piling method, it is necessary to widen the existing footing. In general practice adopted in conventional widening methods, reinforcing bars arranged in the footing are cut, which are then weld-joined with the reinforcing bars in the additionally-installed footing. However, when applying this method, the loading mechanism causes temporary changes due to the cutting of reinforcing bars in the existing footing, which may lead to the occurrence of some tasks to secure structural safety. In addition, because the space required for welding is narrow, there arises the issue of whether welding reliability can be secured.

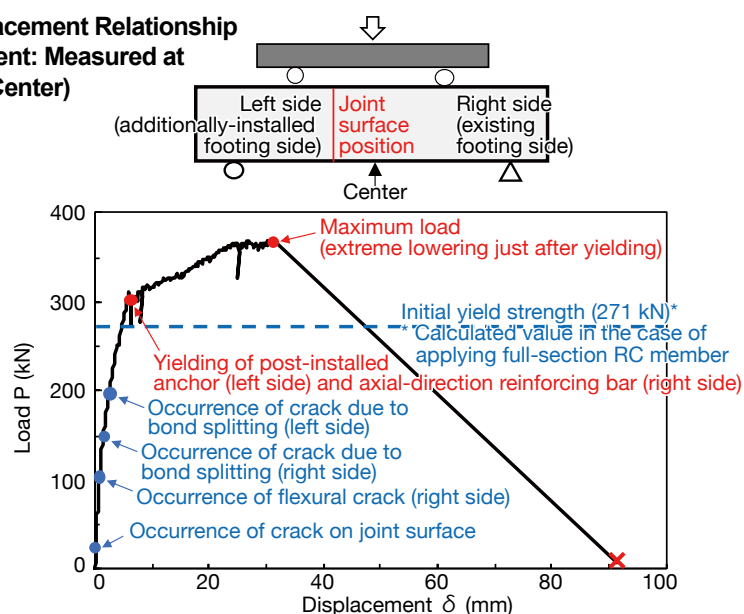
Given such issues, the Public Works Research Institute is promoting the examination of a new footing widening method by which existing and newly-installed footings are rigidly-joined by the use of post-installed anchors. In order to verify the level of footing integration attained by the use of this new footing widening method, a bending test was conducted using an RC specimen as shown in Fig. 1. As a result, it was confirmed that the calculation results based on the assumption of full-section RC members nearly coincided with the load required for the post-installed anchor and the axial-direction

reinforcing bar of the specimen to yield (Fig. 2). On the other hand, there remained the task that brittle fracturing finally occurred in integrated footing due to bond splitting fracture occurring after the yielding of reinforcing bars (Photo 1).

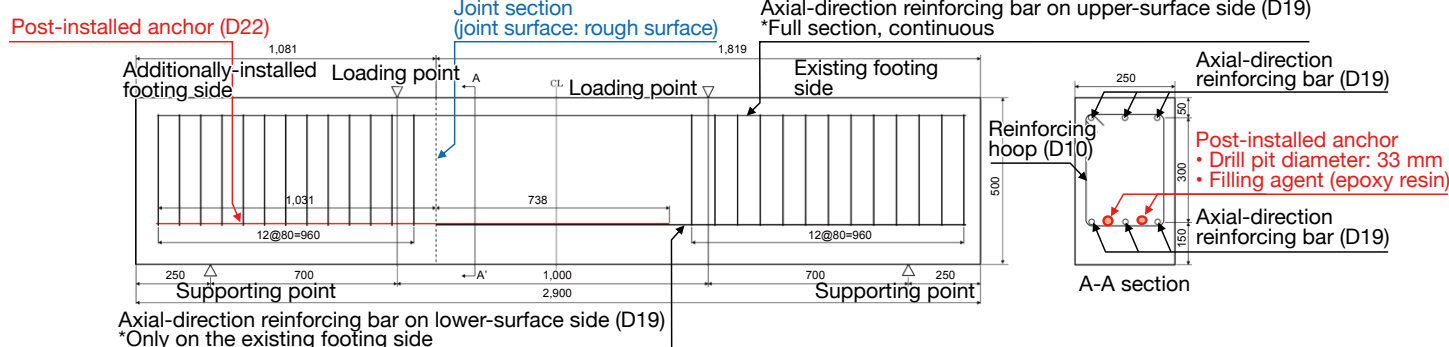


Photo 1 Condition of specimen at the stage of maximum loading

**Fig. 2 Load-Displacement Relationship (Displacement: Measured at Specimen Center)**



**Fig. 1 Dimensions of Specimens (unit: mm) and Detailed Reinforcing Bar Arrangement**



Plans call for further examination pertaining to the relation between the placement positions of existing reinforcing bars and post-installed anchors and the promotion of the research toward the practical application of this new footing widening method.

### Effects of Group Piles on Foundations Reinforced with Additional Piling

In the currently prevailing technical standard (*Specifications for Highway Bridges*)<sup>1)</sup>, the effect on horizontal displacement due to interference between piles is considered as a group pile effect, assuming that all the piles that make up the pile foundation have identical dimensions. However, in the additional piling method, there is a case in which the adoption of piles with a dimension different from that of existing piles becomes more rational because of the difference between the construction method adopted at the initial stage and the additional piling method and also restrictions imposed on the construction site.

Then, in order to make a basic assessment of the group pile effect on a foundation structured with the combined use of piles of different diameters and grades, the Public Works Research Institute carried out a 3D FEM pushover analysis targeting two piles shown in Fig. 3. As shown in Fig. 4, this analysis showed useful results: Specifically, when comparing a foundation with piles having en-

tirely identical diameter and grade (case A) to a foundation with a combination of piles having different diameter and grade (case B), the level of the ground reaction force of the back-row pile at a depth close to the pile head differed between cases A and B, and further the ground reaction force in case B with different pile diameter and grade was larger than that in case A with identical pile diameter and grade.

In the future, we will further promote the verification of the factors affecting the group pile effect such as not only the pile diameter and grade but the interval between piles and ground conditions. The final aim is to establish a general-purpose method to verify the group pile effect.

### Future Tasks

In this additional piling method applied to pile foundation, there remain some

tasks to be solved such as load bearing by new and existing piles and a method to establish the critical state in addition to the tasks explained above. At the Public Works Research Institute, research to solve these tasks is being promoted so as to contribute towards the building of highways that are high in safety and reliability.

### Acknowledgements

Part of the research introduced above was promoted capitalizing on a subsidy from the Japan Iron and Steel Federation, for which we would like to express our sincere gratitude.

### Reference

- 1) Specifications for Highway Bridges (November 2017), Japan Road Association

Fig. 3 Analytical Model

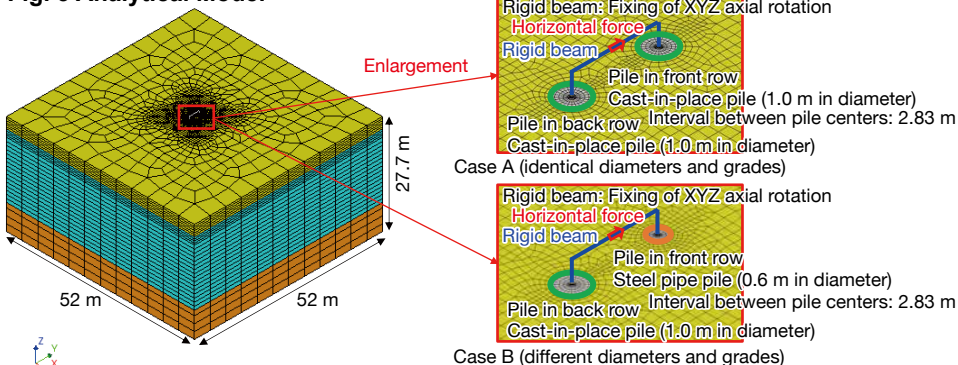
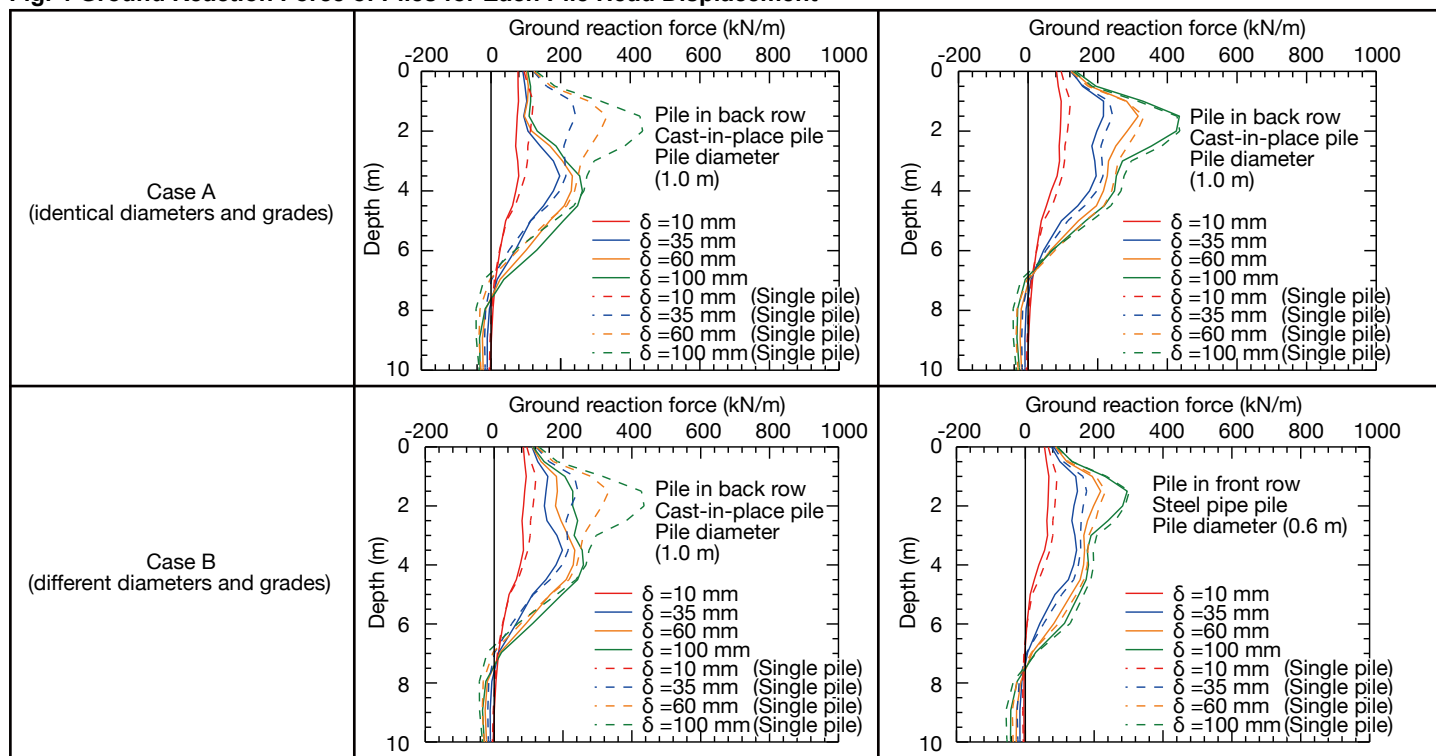


Fig. 4 Ground Reaction Force of Piles for Each Pile Head Displacement





# Model Experiments on Piping Failure of River Levees

**Kiyonobu Kasama**  
Professor, Kyushu University



**Kiyonobu Kasama:** He is currently professor at the Division of Civil and Structural Engineering, Faculty of Engineering, Kyushu University. He received Ph.D. in Civil and Structural Engineering from Kyushu University in 2004. Among his main area of research are experimental and numerical characterization for cement-mixed ground, reliability theory approach to ground improvement and earth reinforcement, and recycling geomaterial to concrete material.

## Aim of Experiment

In recent years, damages arising from river levee failures have occurred due to the continuous rise of river water level caused by heavy rain rainfall. The following three are accepted as the levee collapse mechanisms:

- Piping failure which grows in the foundation ground just beneath a levee structure
- Sliding failure of the levee structure due to the rise of river water levels caused by heavy rainfall
- Erosion and scouring failures due to the overflowing of river water

Because of the intensified heavy rains and continuous rise of river water level, it is anticipated that the multiple failure mechanism will occur.

From these backgrounds, an experiment device was developed that can simulate the three failure mechanisms mentioned above, and a model experiment was conducted by reproducing the piping failure occurring in the foundation ground. In addition, the effectiveness of reinforcement with steel sheet piles on piping failure was verified, and a risk assessment for piping failure was conducted based on the ratio of total weight of covered layer  $G$  to water pressure  $W$  at the piping failure points.

## Experiment Method

An experiment device was composed of a water-level control device, pump, tank, drainage channel, levee and earth tank to produce the foundation ground (Fig. 1). The left side of the device was settled as the river side and the right side as the land inside. The water was supplied using the pump, and the river water level was adjusted using the water level control device. The water flown to land side was returned for circulation via the drainage channel installed at a height similar to that of the foundation ground.

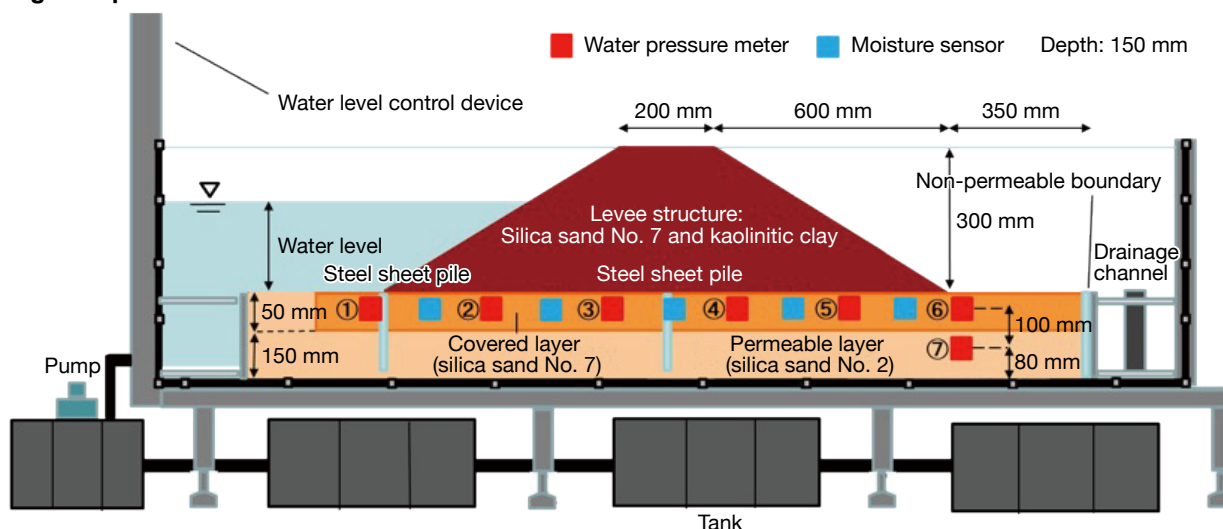
The levee structure was a trapezoid shape having an upper bottom of 200 mm, a lower bottom of 1,400 mm and a height of 300 mm. The dimensions of the foundation ground measured 2,100 mm in length and 200 mm in height. In order to reproduce piping failure, the foundation ground was composed of two layers—a covered layer in the surface layer section and a permeable layer in the lower section with a layer thicknesses of 50 mm and 150 mm respectively. Referring to research by Igami et al<sup>1)</sup>, part of the permeable layer was exposed by 80 mm, and a non-permeable boundary was provided in a position 350 mm from the slope toe of the levee.

The foundation ground was prepared in the following manner: silica sands No. 2 and No. 7 were mixed so that the water content became 5% for each sand, and the sand layer was compacted for every 50 mm using a compaction device. For the levee structure, silica sand No. 7 and kaolinitic clay were mixed so that the water content became 10%, and the soil mixture of silica sand No. 7 and kaolinitic clay was compacted for every 30 mm.

In order to verify the effectiveness of reinforcement by means of the installation of steel sheet piles against piping failure, an experiment was conducted by installing steel sheet piles, whose installation length is 90% of the foundation ground thickness, at the slope toe on land side of the levee and at the center of the levee structure.

As for the experiment procedure, water was passed through the foundation ground and it was confirmed with a moisture sensor that the foundation ground caused sufficient saturation, then the water level was raised by 6 mm/min using the water level control device as shown in Fig. 2. After the water level reached 300 mm, it was confirmed whether or not piping failure occurred, while maintaining the water level for 10 minutes. In addition, the ratio of the

**Fig. 1 Experiment Device**



total weight of covered layer  $G$  to water pressure  $W$  at the bottom of covered layer was calculated employing the pore water pressure measured during the experiment.

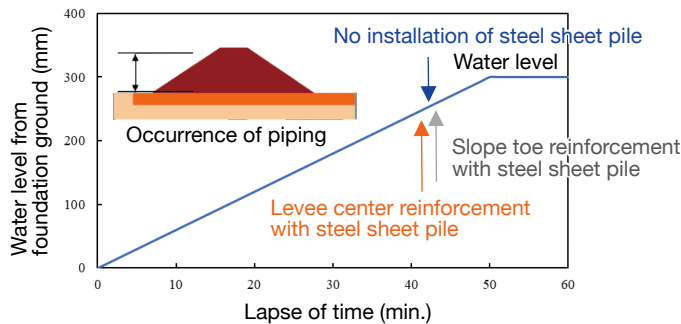
Fig. 2 shows the relationship between the lapse of time and the water level. It also shows the time of occurrence of piping failure confirmed through visual observation. Piping failure occurred after a lapse of 42 minutes in the case of no installation of steel sheet piles, 43 minutes in the case of slope toe reinforcement with steel sheet piles and 41 minutes in the case of levee center reinforcement with steel sheet piles, and thus it was impossible to prevent piping failure from occurring even by installing steel sheet piles. However, the size of the piping hole was reduced to about 30%.

Fig. 3 shows the water pressure of the permeable layer observed in the case of no installation of steel sheet piles, slope toe reinforcement with piles and levee center reinforcement with piles. In the case of slope toe reinforcement with steel sheet piles, the water pressure decreased by about 75% from the case of no installation of piles, and also in the case of levee center reinforcement with piles, the water pressure decreased by about 50% from the case of no installation of piles. These large decreases are considered attributable to the narrowed sectional area for water flow and reduced amount of the seepage flow attained by the installation of steel sheet piles.

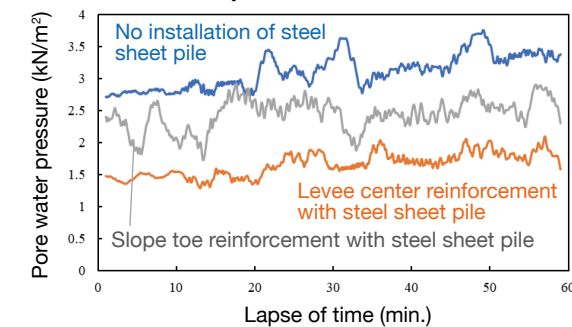
In addition, the water pressure in the case of slope toe reinforcement with piles reached about 70% of that in the case of levee center reinforcement with piles. This is considered attributable to levee center reinforcement with piles being closer to the location of piping failure, where the effect of steel sheet pile installation on the reduction of seepage flow was more pronounced.

Fig. 4 shows  $G/W$ , a risk level for the occurrence of piping failure calculated using the measured water pressure. The value  $G$  was calculated by setting the unit saturated volume weight at 19.29 kN/m<sup>3</sup> and the covered layer thickness at 0.05 m, which led to a value of 0.96 kN/m<sup>2</sup>. The value  $W$  was calculated by the use of the water pressure measured at the position of the covered layer bottom surface. It is understood from the figure that the value  $G/W$  decreased with the lapse of time. The value  $G/W$  at the stage of the occurrence of sand blasting in the case of no installation of steel sheet piles was 1.11, and in the case of levee center reinforcement was 1.31, and further,  $G/W$  in the case of the covered layer bottom surface showed a value close to 1.

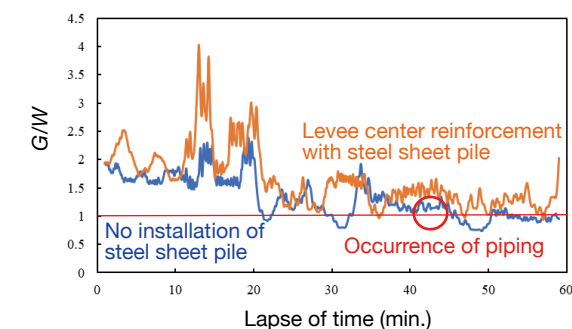
**Fig. 2 Relationship between Lapse of Time and Water Level**



**Fig. 3 Water Pressure of Permeable Layer just beneath Slope Toe inside Levee**



**Fig. 4 Comparison of  $G/W$  Values**



It was shown from these values that the condition of the occurrence of piping failure and its timing can quantitatively be verified by the use of the value  $G/W$ . As a cause attributable to the value  $G/W$  not falling short of 1, it is considered that the water pressure  $W$  dispersed widely. To that end, it is necessary to improve the measurement accuracy.

### Useful Experiment Results

The following results were obtained from the model experiments.

- An experiment device was developed that could reproduce three major collapse mechanisms for river levees: piping failure at the foundation ground, sliding failure of the levee structure and erosion/scouring failure due to overflowing.
- In reinforcement with steel sheet piles that cut off the foundation ground by 90%, as applied in this experiment, it

was impossible to prevent piping failure from occurring regardless of the steel sheet pile installation position. However, the size and scale of the piping hole could be reduced to 30%.

- The risk level of the occurrence of piping failure was judged using the  $G/W$  obtained based on the total weight of the covered layer  $G$  and the measured water pressure  $W$ . The measurement variation of water pressure  $W$  was large, and it is necessary to improve measurement accuracy in the future, but there is a possibility that risk assessment involved in piping failure can be carried out using  $G/W$ .

### Reference

- 1) T. Igami, K. Maeda, Y. Maki and R. Okada: Suppression effect of piping progress in river levee by sheet-pile installation, The 33rd JGS Chubu Ground Engineering Symposium, 2021

# Low-carbon Measures in the Life Cycle of Concrete Structures

**Akio Kasuga**  
Executive Fellow, Sumitomo  
Mitsui Construction



Dr. Akio Kasuga is an Executive Fellow of Sumitomo Mitsui Construction and also a Senior Principal Researcher of the University of Tokyo. He has been designing and building many bridges and has developed many new bridge technologies. He received Trophy Eugene Freyssinet 2013 and Albert Caquot Prize 2021 of AFGC from France. He was the President of fib (Fédération internationale du béton) from 2021 to 2022. He was awarded as the Honorary President of fib in 2023.

## Introduction

According to European data, 60% of cement is used in structural concrete<sup>[1]</sup>. Concrete emits 2.8 billion tons of CO<sub>2</sub> per year worldwide, so if the ratio were the same as in Europe, cement in structural concrete would emit 5.2% of the amount of CO<sub>2</sub> emitted by mankind in a year. We cannot just wait for these materials to go zero carbon. The countdown to carbon neutrality has already begun. The author explained how carbon neutrality will affect concrete structures<sup>[2]</sup>.

This paper will present low-carbon and decarbonisation technologies in the supply chain of concrete structures that can be applied today and those that need to be developed in the future to achieve carbon neutrality by 2050 and will pres-

ent possible concrete measures that could be taken.

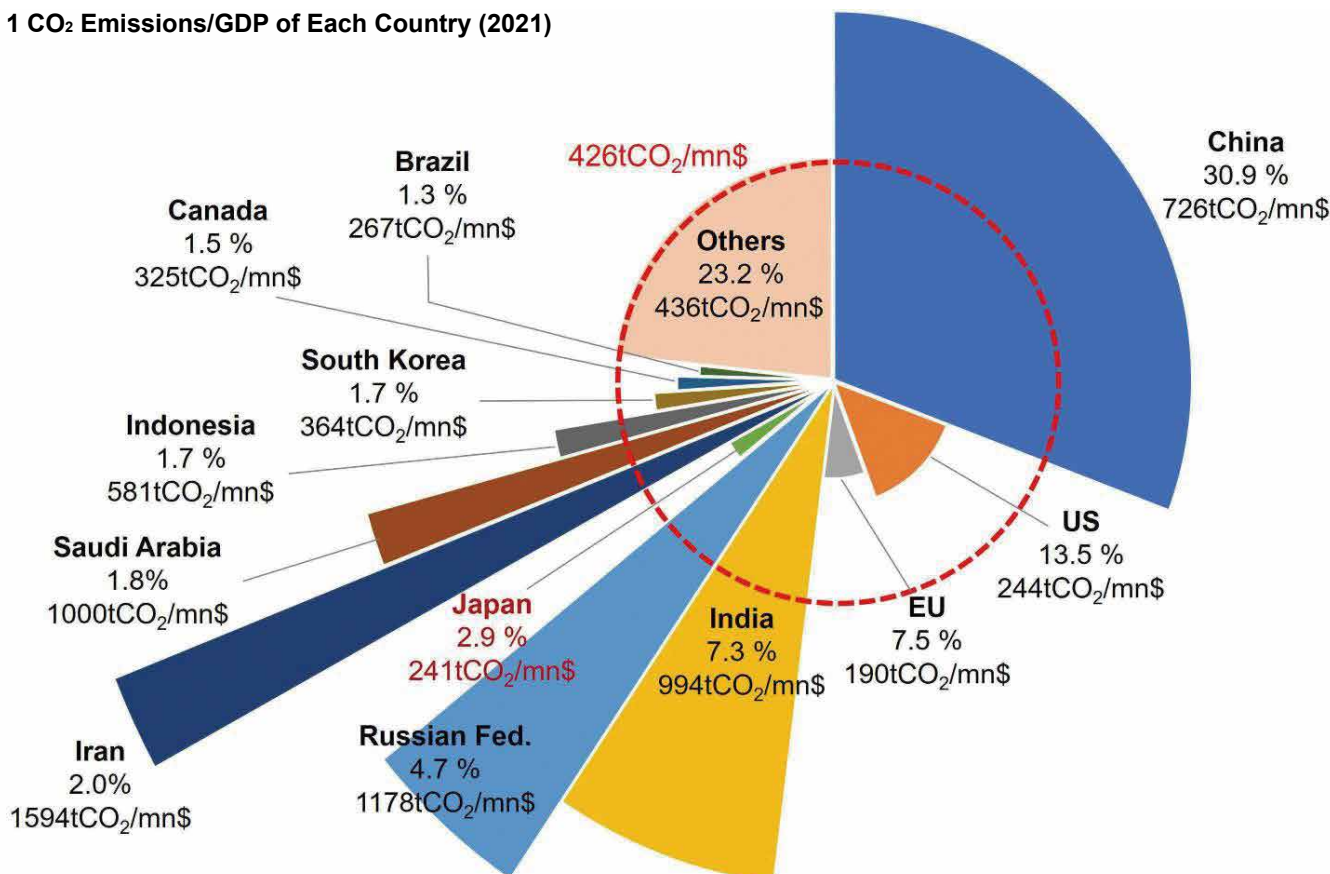
## Economic Implications of Carbon Neutrality

To begin with, consider how much it would cost to go carbon neutral in 2050. This is not a particularly difficult calculation. If emissions of 32.5 billion tCO<sub>2</sub> per year were to be reduced at a constant rate for 30 years, it would amount to about 500 billion tCO<sub>2</sub>. Multiply this by an assumed average carbon pricing of 12,000 yen/tCO<sub>2</sub>, and the result is 6,000 trillion yen<sup>[3]</sup>. This is a tremendous amount of money, but the IPCC subsequently announced that a maximum of \$30 trillion would be required to halve carbon emissions<sup>[4]</sup>. This is equivalent to the author's

estimate. Bill Gates defined a green premium of \$5.1 trillion/year by multiplying 51 billion tons of annual greenhouse gas emissions by \$100<sup>[5]</sup>.

Fig. 1 shows the CO<sub>2</sub> emissions<sup>[6]</sup> of each country in 2021 divided by its GDP<sup>[7]</sup>. The global average is 426 tCO<sub>2</sub>/million \$ (red dotted line), which means that China, India, Russia, Iran, Indonesia, Saudi Arabia and South Africa have high CO<sub>2</sub> emissions relative to their economic size. The CO<sub>2</sub> emissions divided by the money index is a key factor in the argument of this paper. There is still a lot of data to be developed on the CO<sub>2</sub> footprint of structural concrete. And when considering strategies to decarbonise and reduce the carbon footprint of structural concrete, the answer that it cannot be do-

Fig. 1 CO<sub>2</sub> Emissions/GDP of Each Country (2021)





ne because of a lack of data is a missed opportunity. Such a comprehensive indicator will help us make decisions towards carbon neutrality.

CO<sub>2</sub> Emissions of Structural Concrete

Fig. 2 shows the EN15978 construction supply chain in Europe. And the CDP (Carbon Disclosure Project) classification of each area of the construction supply chain is shown below. Scope 1 and 2 CO<sub>2</sub> emissions need to be reduced un-

der the responsibility of the key players. However, as long as they are integrated into the supply chain, Scope 3 must also be addressed in some way in each area. In particular, designers will be involved throughout the LCA and therefore proposals for low-carbonisation and decarbonisation will be required from operators in the LCA.

According to the construction companies' data disclosed by the CDP, the indicator of annual CO<sub>2</sub> emissions divided by their turnover is 98% Scope 3 with 1000

tCO<sub>2</sub>/100 million yen (Table 1). The construction stage of A4 and A5, Scope 1 and 2 for construction companies, is only 2% in the case of Japan. Most of the CO<sub>2</sub> in the construction supply chain is emitted during the material production stage from A1 to A3 and the use stage from B1 to B5. The former is Scope 1, 2 of the material supplier and the latter is Scope 1, 2 of the operator. According to a construction company to which the author belongs, 400 tCO<sub>2</sub>/100 million yen from A1 to A3 emits about 40% of CO<sub>2</sub>, and

Fig. 2 Scope of CO<sub>2</sub> Reductions to Be Addressed in Construction and Areas of the Construction Supply Chain

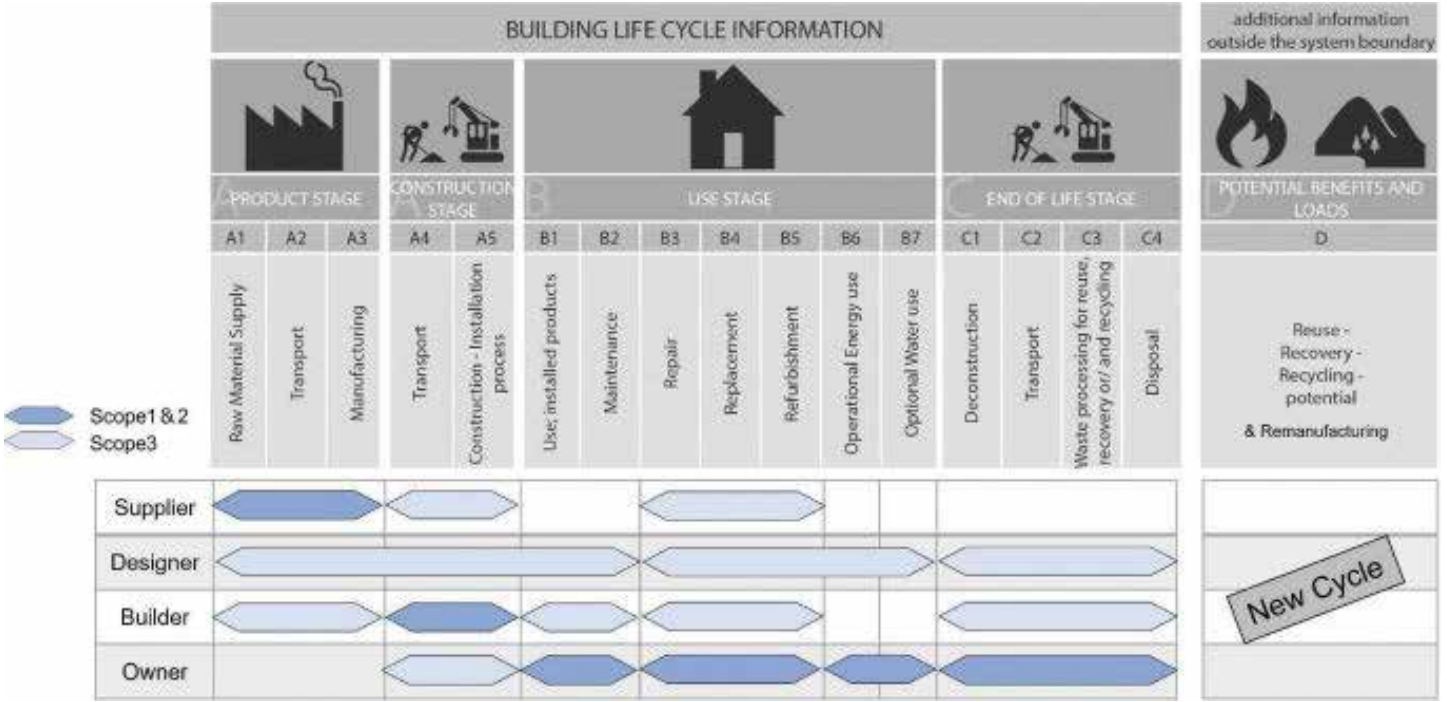


Table 1 CO<sub>2</sub> Emissions by Japanese Industry (calculated by author from CDP data)

Industry	Scope 1 and 2	Scope 3
Construction	25	1,080
Real estate	90	270
Internet service	12	110
Finance	5	13
Fund	300	260
Chemical materials	470	830
Transportation (railroads)	290	200
Transportation (vehicles)	50	90
Transportation (ships)	1,220	160
Transportation (aviation)	1,720	460
Retail	30	1,070
General trading	80	350
Manufacturing (electrical equipment)	70	3,370
Manufacturing (industrial equipment)	50	920

600 tCO<sub>2</sub>/100 million yen from B1 to B5 emits about 60% of CO<sub>2</sub>. Therefore, A1 to A3 and B1 to B5 CO<sub>2</sub> emission reduction is an important key.

Here is an interesting database. Fig. 3 shows the relationship between CO<sub>2</sub> emissions and construction costs for bridge construction in the UK<sup>[8]</sup>. Although there are some differences among road bridges, railroad bridges, and pedestrian bridges with different loads, a good correlation is shown, and the gradient is approximately 400 tCO<sub>2</sub>/million €. Despite the influence of prices and exchange rates, it can be said to be at the same level as the 400 tCO<sub>2</sub>/million € of A1 to A3 shown earlier. We believe that

these facts indicate that CO<sub>2</sub> emissions are closely related to economic activities. The indicator of 400 tCO<sub>2</sub>/million € or 400 tCO<sub>2</sub>/100 million yen is a useful indicator to consider now for future strategies for reduction, as the CO<sub>2</sub> emissions database in the LCA for structural concrete is currently insufficient.

### Low-carbon Technologies at the Material Manufacturing Stage

The relationship between the durability of structural concrete and CO<sub>2</sub> emissions is shown conceptually in Fig. 4 (a). As shown in Fig. 4 (b), we must aim to reduce CO<sub>2</sub> emissions at all stages. The first step is to deal with the material

manufacturing stage. Until steel and cement achieve zero-carbon status, the A1 to A3 stages must be low-carbon. There are already many studies and achievements in concrete where cement is replaced by by-products. Of course, it is not possible to substitute all of the current cement with by-products, but it is a transitional measure until zero-carbon cement is achieved. In addition, since low-carbon concrete is slow to develop strength, steam curing is required for precast products due to restrictions on the use of formwork diversion. However, steam curing using boilers emits the same amount of CO<sub>2</sub> in exhaust gas as that reduced by the concrete itself, so it is necessary to consider the reuse of CO<sub>2</sub> through CCUS or other means.

Furthermore, since low-carbon concrete has a lower alkalinity than normal concrete, it can be said to be a neutralized concrete from the beginning. Therefore, some measures that do not deteriorate the reinforcing steel are necessary to prevent the durability of the concrete. And when low-carbon concrete is used in structures, the issue is strength. There are examples of concrete without cement that has achieved a strength of over 100 MPa<sup>[9]</sup>, and this technology can reduce CO<sub>2</sub> emissions by about 70% (Photo 1).

### Low-carbon Technologies in the Use Stage

In order to reduce CO<sub>2</sub> emissions during the use stage shown in Fig. 4 (b), data on the relationship between durability and LCA, as well as data on conservation by operators, are indispensable. However, this type of data is currently very scarce and must be accumulated in the future. The biggest issue in maintenance is how to prevent the deterioration of reinforcing steel. The high durability of structural concrete is important to reduce CO<sub>2</sub> emissions during the use stage. Currently available technologies such as stainless steel, aluminum reinforcement, or steel bars with anti-corrosion coating can be used for this purpose. However, the use of reinforcing steel in low-carbon concrete is still a subject of limited knowledge and must be studied further. Importantly, even if steel and cement achieve zero-carbon status, durability and CO<sub>2</sub> emissions at the use stage will remain an issue.

Increasingly, FRPs such as carbon, aramid, and basalt are being used for reinforcement. The world's first non-metal-

**Fig. 3 CO<sub>2</sub> Emissions in Bridge Construction (processed based on Reference 8)**

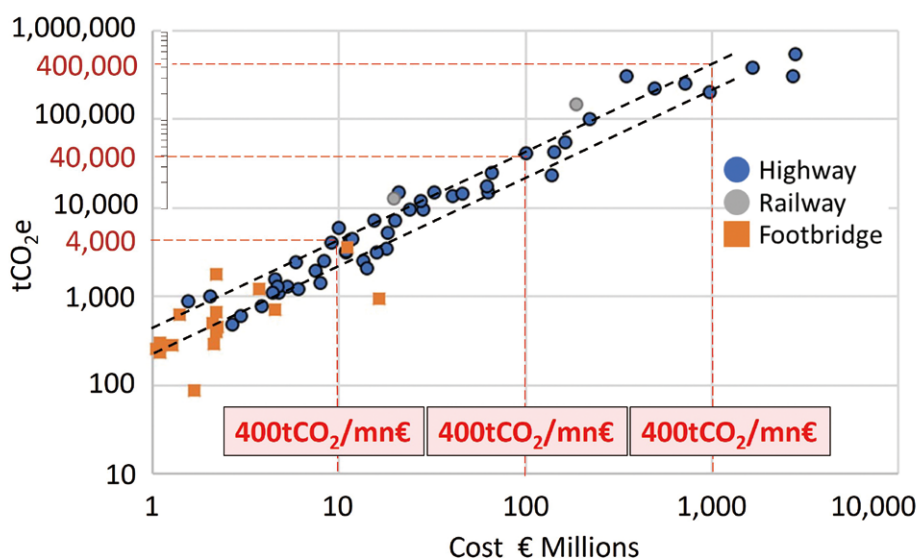
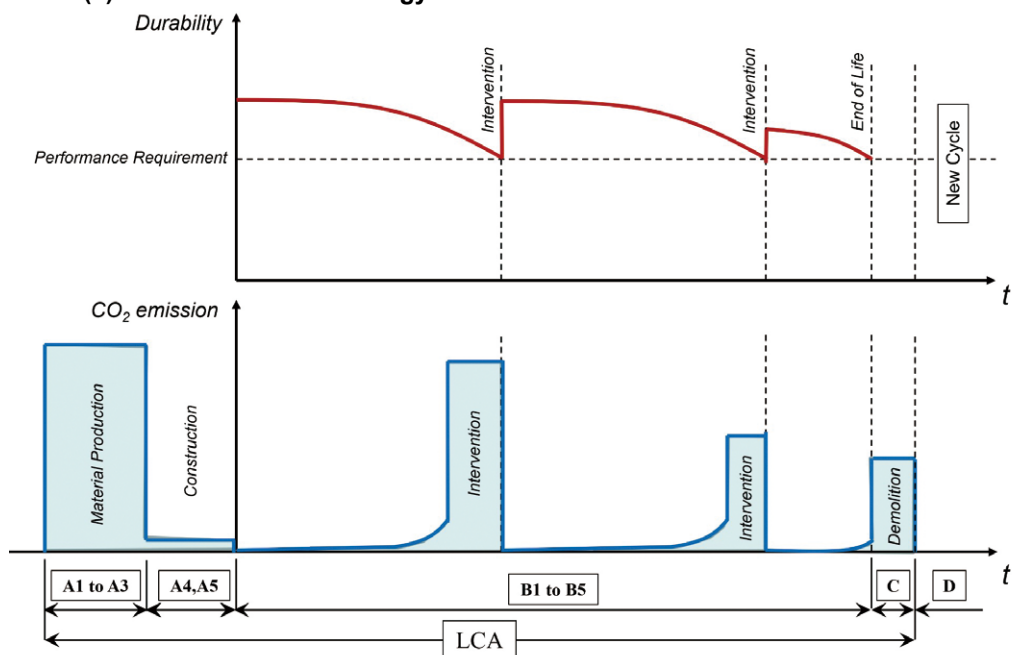


**Fig. 4 Concept of Durability and CO<sub>2</sub> Emissions**

**(a) Conventional Technology**



**(b) Low-carbon Technology**

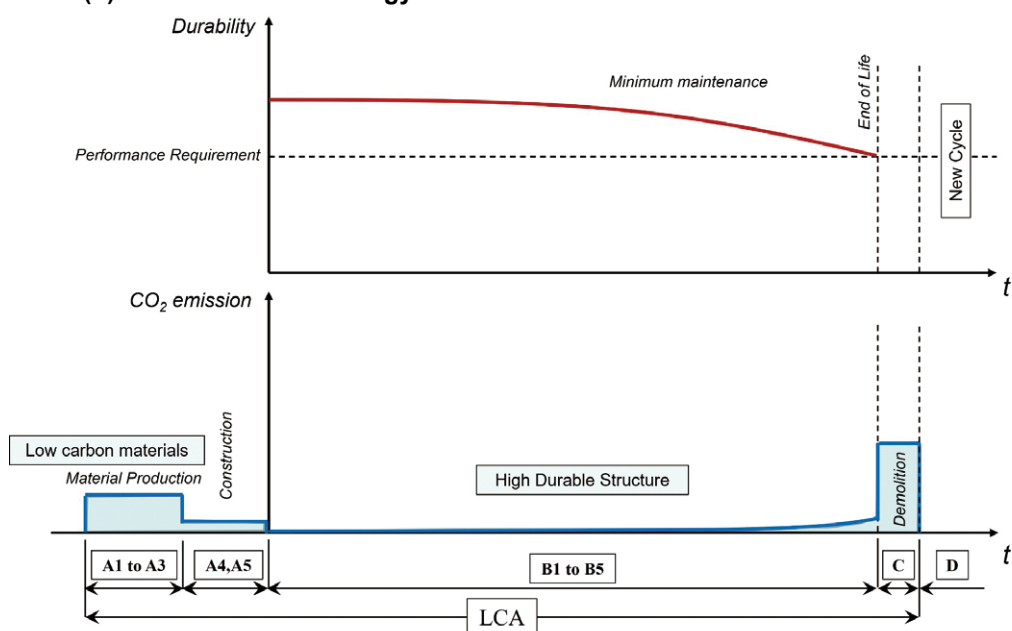


Photo 1 Zero cement concrete



lic bridge with aramid FRP prestressing tendons was built as a motorway in 2020 (Photo 2)<sup>[10]</sup>, and non-metallic decks were built using the same technology in 2021 (Photo 3). These materials can remove deterioration factors from structural concrete and are compatible with low-carbon concrete with low alkalinity. FRP can be used as a tendon to provide prestressing forces as well as reinforcement. Estimates using American Association of State Highway and Transportation Officials (AASHTO) girders show that the combination of zero cement concrete, aramid FRP tendons, and nonmetallic technology of GFRP reinforcements can reduce CO<sub>2</sub> emissions by 82% in LCA compared to conventional technology (Table 2)<sup>[2]</sup>,<sup>[11]</sup>. In addition, a pretensioned girder combining high-strength zero-cement concrete and aramid tendons was constructed in 2019 (Photo 4). This girder has reduced CO<sub>2</sub> emissions by about 75% compared to conventional technologies in LCA (Fig. 5)<sup>[12]</sup>. These low-carbon technologies will be valued at a carbon price for the reduced CO<sub>2</sub> emissions if a carbon tax is introduced in Japan in the future. And the carbon credit market becomes as large as in Europe. This will be a great motivation for technology development.

### Low-carbon Technologies That Contribute to the Circular Economy

The life cycle of concrete structures is long and involves social and environmental changes during the use stage. In other words, changes in population, climate, and technological paradigm shifts are expected to force changes in the function of the structure. It is important to design the first cycle with the expectation of minimizing CO<sub>2</sub> emissions at that time.

Concrete structures that are easy to dismantle and reuse the dismantled components can reduce CO<sub>2</sub> emissions from A1 to A3 to as close to zero as possible<sup>[2]</sup>. Various technologies related to multi-cycle concrete structures are issues to be addressed in the future, including standards. They include new challenges such as in-service monitoring, evaluation of components after dismantling, technologies to remanufacture them equivalent to new ones, and standardization of structures. In the Netherlands, the “Bridge Bank”<sup>[13]</sup>, a governmental bridge reuse program, is already in place as a multi-cycle attempt, and it is very interesting.



Photo 2 World's first non-metallic bridge (Bessodani Bridge)

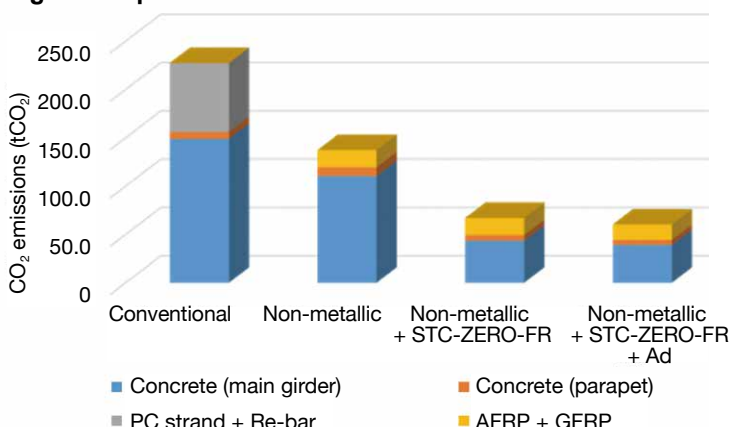


Photo 3 Non-metallic deck (Tadenodaini Bridge)



Photo 4 Fusion of zero-cement concrete and non-metallic technology

Fig. 5 Comparison of CO<sub>2</sub> Emissions<sup>[12]</sup>



**Table 2 Probabilistic Estimation of Whole Life tCO<sub>2</sub> of the BT-72 Girder Bridge Superstructure<sup>[11]</sup>**

	Lifecycle factor	tCO <sub>2</sub>				Whole life emission rate (tCO <sub>2</sub> /m <sup>3</sup> )	tCO <sub>2</sub> reduction (%)
		Stage A		Stage B and Stage C	(A+B+C)		
		A1-A3 (80% of A)	A4-A5 (20% of A)				
Conventional bridge	Repair and replacement	174	43	326 (1.5 times of A)	543	2.2	NA
Next-generation bridge	No repair and replacement	70	18	4.5 (12% of whole life emission)	100	0.4	82

### Toughening in the Use Stage

Disasters such as earthquakes and floods not only cause significant economic losses, but also emit large amounts of CO<sub>2</sub> due to debris disposal and reconstruction. In 2018, the Japan Society of Civil Engineers (JSCE) published a forecast of economic, property, and financial damage from a possible major disaster<sup>[14]</sup>. For example, for an earthquake directly under the Tokyo metropolitan area, which is said to have a 70% probability of occurring within the next 30 years, they forecast economic damage of 731 trillion yen, asset damage of 47 trillion yen, and financial damage of 77 trillion yen. Based on this data, CO<sub>2</sub> emissions estimate due to an earthquake directly under the Tokyo metropolitan area was then made. Assuming that the cost of reconstruction is equivalent to the asset damage, the reconstruction cost of 47 trillion yen is multiplied by 400 tCO<sub>2</sub>/100 million yen, the index shown above, to derive 1.9 billion tCO<sub>2</sub>. This is equivalent to 16% of Japan's annual CO<sub>2</sub> emissions, or 3% extra CO<sub>2</sub> emissions every year if reconstruction is completed in five years.

At the same time, JSCE has also shown that a 34% reduction in disaster mitigation is possible if more than 10 trillion yen of seismic retrofitting of infrastructure is implemented against an earthquake directly under the Tokyo metropolitan area. In other words, CO<sub>2</sub> emissions could also be reduced. Disasters are events in the use stage. In other words, reducing CO<sub>2</sub> emissions here is Scope 1 and 2 for operators. The huge cost can be financed by private funds. It is known that a pay for success type fund can be established as a SIB (Social Impact Bond)<sup>[15], [16]</sup>. The amount of CO<sub>2</sub> emissions from the disposal of disaster debris can also be roughly calculated, but it is only a few percent of that of reconstruction. Private-sector funds invested in the strengthening of this use stage will significantly reduce CO<sub>2</sub> emissions, making it the feasible ESG investment.

### Conclusions

For concrete structures, which alone account for 6% of global CO<sub>2</sub> emissions from major materials, the cost of achieving carbon neutrality by 2050 will be significant. However, depending on whether this is seen as a cost or a value, the actions will be very different. The technologies that will contribute to carbon neutrality in structural concrete are largely the result of our innovation. In other words, it is not a risk but an opportunity<sup>[12]</sup>. The value attached to CO<sub>2</sub> reduction means that low carbon and decarbonisation technologies will be properly paid for and will attract investment in these new technologies. However, these new technologies need to be fairly verified by a third party. The ESG investments that are now making headlines will increasingly be in valuable technologies that are not greenwashed.

As part of the move towards carbon neutrality, *fib* (Fédération internationale du béton) has initiated a special activity group to build a useful platform for its members by filling in the missing data on the use stage and combining it with a materials footprint database. This is a major move that spans the entire organisation, and the main players are the next generation of young people. Although the movement in Japan is still slow, I hope that what I have described above will help you in the future.

### References

- [1] Favier A., De Wolf C., Scrivener K. and Habert G., A sustainable future for the European cement and concrete industry, ETH, EPFL, 2018
- [2] Kasuga, A., Impact of carbon neutrality on structural concrete – Not a risk but an opportunity, *fib* Structural Concrete, 2012, pp1725-1736
- [3] Kasuga, A., The “Anthropocene” bill as indicated by CO<sub>2</sub>, Nikkei, 24 June 2021 (In Japanese)
- [4] Climate Change 2022: Impacts, Adaptation and Vulnerability, IPCC, Au-

gust 2022

- [5] Gates B., How to avoid a climate Disaster, Knopf, 2021 Feb
- [6] Ritchie H., Roser M., CO<sub>2</sub> emissions, Our World in Data, 2017 May (last revised 2020 Aug.), Available from: <https://our-worldindata.org/co2-emissions#global-co2-emissions-from-fossil-fuels-and-land-use-change>
- [7] The World Bank open data. GDP (current US\$), <https://data.worldbank.org/indicator/NY.GDP.MKTP.CD>
- [8] Collings D., The carbon footprint of bridges. Structural engineering international, 2021 May
- [9] Matsuda T., Mine R., Geddes D., Walkley B. and Provis J., Development of ultra-low shrinkage and high strength concrete without Portland cement with experimental study on its fabrication, *fib* Oslo Congress, 2022 Jun
- [10] Matsuo Y., Wada Y., Fujioka T and Nagamoto N., Construction of non-metal bridge, *fib* Symposium in Lisbon, 2021 June
- [11] Zerín A. and Kasuga A., LCA of a challenging low carbon ultra-high durability non-metallic bridge, *fib* Congress 2022 in Oslo, 2022 June
- [12] Shinozaki H., Matsuda T. and Kasuga A., Construction of non-metallic bridge using zero-cement concrete, *fib* Congress 2022 in Oslo, 2022 June
- [13] <https://www.nationalebruggenbank.nl/en/>
- [14] Report on Technical Study on Countermeasures for Mega Disasters Causing “National Disaster”, Japan Society of Civil Engineers, 2018 (in Japanese)
- [15] Kamatani, T., et al., A study on PFS (Pay for Success) investment in development of infrastructure for disaster prevention, Policy and Practice Studies, Volume 7, Number 1, 2021 (in Japanese)
- [16] Recommendations on Social Implementation of Disaster Mitigation SIB for Private Sector Financing of Disaster Mitigation Investments, Disaster Mitigation Infrastructure PFS Study Group, Resilience Japan Promotion Council, April 2022 (in Japanese)



# AJSI Webinar 2024: Achieving Carbon Neutrality in the Steel Sector

The Japan Iron and Steel Federation (JISF) concluded a memorandum with the ASEAN Iron and Steel Council (AISC) in fostering interaction concerning the environment, standardization and trade in May 2014.

In the field of environment, JISF has launched a public-private collaborative scheme called the ASEAN-Japan Steel Initiative (AJSI) with the cooperation of the Ministry of Economy, Trade and Industry. The purpose of this initiative is to provide a platform to exchange knowledge and experiences, thereby contributing to energy saving & environmental protection in ASEAN countries. In addition, AJSI aims to encourage technology transfer from Japan to the ASEAN steel industry. To achieve this goal, JISF has established three main activities: Steel Plant Diagno-

sis, Technologies customized List and Public and Private Collaborative Workshop.

On February 6, 2024, as Public and Private Collaborative Workshop, JISF held an online seminar “AJSI Webinar 2024: Achieving Carbon Neutrality in the Steel Sector” targeting ASEAN countries, to which a total around 180 participants from the government, steelmakers and others in those nations participated.

Reflecting the growing pressure for decarbonization, this webinar focused on Carbon Neutrality, introducing policies and initiatives of both the public and private sector.

JISF also incorporated items such as programs for overseas human resource development by ECCJ and best practice of an EAF company, in response to the feedback survey from last year. The we-

binar also provided information on Japan's Policies towards Green Transformation. Not only did we welcome the steel companies of Japan, but we also had Thailand and Indonesia steel makers to have an informative presentation on their initiatives towards Carbon Neutrality.

South East Asia Iron and Steel Institute (SEAISI) expressed gratitude for the contribution of the past AJSI activities, and also shared the view that the continuous cooperation between Japan and ASEAN countries, which shares the same goal of carbon neutrality, is truly meaningful.

JISF, together with the Japanese government, will continue to support energy efficiency and environmental protection in the ASEAN steel industry and cherish the long-term relationship between Japan and ASEAN countries fostered through AJSI.

## Courtesy Visit to TISI and the FY2023 Japan-Thailand Steel Cooperation Program

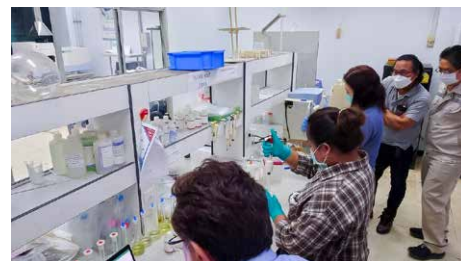
Since 2008, the Japan Iron and Steel Federation (JISF) has initiated technical cooperation programs in Thailand's steel sector under the Japan-Thailand Economic Partnership Agreement (JTEPA). Since 2017, JISF has been providing the technical cooperation program to the Thai steel industry between JISF and the Iron and Steel Institute of Thailand (ISIT) on an annual basis. The program mainly involves the standardisation of steel product in Thailand, including formulation of steel product standards in Thailand and technical guidance to strengthen a quality inspection system of the testing laboratory owned by ISIT.

In July 2022, a Memorandum of Understanding (MoU) was signed between JISF, the Thai Industrial Standards Institute (TI-

SI) and ISIT. Under this agreement, TISI gained permission to use the copyright of Japanese Industrial Standards (JIS) held by the JISF Standardisation Centre. The MoU also established a contact point on both sides for exchanging operational information regarding TIS's mandatory standards. Approximately a year later, on 29 May, JISF paid a courtesy visit to TISI to discuss the MoU's implementation and mutual trade concerns. The update and formulation of new TIS mandatory standards were also discussed. The meeting concluded with confirmation of ongoing friendly relations and future technical cooperation between JISF, TISI and ISIT.

Under the steel technical cooperation program in FY2023, JISF conducted a technical guidance by the Japanese experts

to the ISIT Testing Laboratory which covered analysis of coating layer, appropriate use of the testing equipment and management system in Bangkok in May 2024 together with a seminar on JIS steel standards such as Plated Steel Sheets and Strip, Pre-painted Sheet and Strip and Steel Tubes for general/mechanical structure for TISI officials and ISIT member companies by the experts of JISF's Standardisation Centre.



### STEEL CONSTRUCTION TODAY & TOMORROW

© 2024 The Japan Iron and Steel Federation/Japanese Society of Steel Construction

Published jointly by

**The Japan Iron and Steel Federation**

3-2-10, Nihonbashi Kayabacho, Chuo-ku, Tokyo 103-0025, Japan

Phone: 81-3-3669-4815 Fax: 81-3-3667-0245

URL <https://www.jisf.or.jp/en/index.html>

**Japanese Society of Steel Construction**

3F Aminosan Kaikan Building, 3-15-8 Nihonbashi, Chuo-ku, Tokyo 103-0027, Japan

Phone: 81-3-3516-2151 Fax: 81-3-3516-2152

URL <http://www.jssc.or.jp/english/index.html>

Edited by

**Committee on Overseas Market Promotion, The Japan Iron and Steel Federation**

Chairman (Editor): Shunsuke Usami

Published three times per year, **STEEL CONSTRUCTION TODAY & TOMORROW** is circulated to interested persons, companies and public organizations to promote a better understanding of steel products and their application in the construction industry. Any part of this publication may be reproduced with our permission. To download content (PDF format), please go our website at: <https://www.jisf.or.jp/en/activity/sct/index.html>. We welcome your comments about the publication and ask that you contact us at: [sunpou@jisf.or.jp](mailto:sunpou@jisf.or.jp).